Report: LLNL-TR-2011238

Resonance Self-Shielding: Why it is so Important

by
Dermott E. Cullen
1466 Hudson Way
Livermore, CA 94550
Tele: 925-321-4177
E.Mail: RedCullen1@comcast.net
Website: http://redcullen1.net/homepage.new

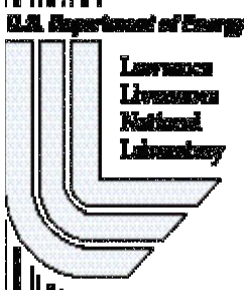

July 28, 2025

DISCLAIMER

This work performed under the auspices of the U.S. Department of Energy by Lawrence Livermore National Laboratory under Contract DE-AC52-07NA27344.

Report: LLNL-TR-2011238

Resonance Self-Shielding: Why it is so Important

by
Dermott E. Cullen
1466 Hudson Way
Livermore, CA 94550
Tele: 925-321-4177
E.Mail: RedCullen1@comcast.net
Website: http://redcullen1.net/homepage.new

July 28, 2025

Contents

Prologue

This paper is one of a series that I am writing to document my 58 years of experience with ENDF and Neutron Transport calculations, beginning when I worked at the National Nuclear Data Center (NNDC), Brookhaven National Laboratory (BNL), from 1967 to 1972. During those years I was the head of the computer unit of NNDC, assigned to develop computer codes to pre-process, view and test ENDF/B data. Since then, I have continued to support the ENDF effort without any official position or monetary compensation, because I realized how important accurate nuclear data is for use in use in our Engineering applications. It is so important to realize that **regardless of how accurate or even perfect our application codes may be to transport particles, without accurate nuclear data we are in a "Garbage In = Garbage Out" situation.**

During these 58 years we have seen a tremendous improvement in the nuclear data available for our use in our **Engineering Applications**. This was to a large degree because of the ENDF format and conventions uniquely defined in what I call the **ENDF Bible, ENDF-102**; it has served as a bridge between evaluators, who produced the data, and engineers who use the data, and most importantly is that users test the data, and supply feedback to the evaluators to further improve the next version of ENDF/B. The close coupling has always been imperative through each version of ENDF/B; today the most recent release is ENDF/B-VIII.1.

The problem that I see is that ENDF/B has been so successful that by about ENDF/B-V or VI, most, if not all, of our **Engineering** needs had been met and users lost interest in further changes, testing and feedback. Since then, I fear rather than striving to meet our Engineering needs, evaluators have been moving away from the intended **Engineering** purposes of ENDF, toward their own personal **Physics** interests. I cannot stress this enough: **ENDF-102 is an Engineering Users Manual, not a Physics Textbook.** Rather than obeying the very strict uniquely definitions and rules in ENDF-102, that meet our Engineering needs, I fear today's evaluators are trying to improve the data using more up-to-date advanced physics. **This may be better Physics, but it is not necessarily better Engineering – and sorry to point out, it is often NOT WHAT WE REQUIRE/NEED FOR OUR ENGINEERING APPLICATIONS.**

I must mention that one of the biggest contributors to the success of ENDF is the supporting software, designed to accurately transform the ENDF evaluated ENDF data from the form it is distributed by data centers, such as NNDC, to the form that it is actually used is our **Engineering applications**. After almost 60 years of development and continued support when I add up all of the salaries and computer costs, by now I estimate that over a billion dollars U.S., has been invested in developing and continuing to maintain these processing and application codes. Needless to say, these codes are very complicated and designed to strictly follow ENDF-102 rules and definitions. This means making even the smallest changes for the sake of **physics,** that you may think is improving an evaluation, can in fact completely destroy the unique interpretation of our **engineering** application codes. Unfortunately, since about ENDF/B-V or VI, this is what I have watched each version of ENDF do; maybe each version of ENDF/B is using **more advanced physics** but unfortunately in my opinion it is moving away from accurately and uniquely defining ENDF-102 compliant data, for use in our **Engineering applications**. How can this be happening?

What came as a shock to me is that when I recently asked several physicists who today create ENDF/B evaluated data, they admitted they were not familiar with Doppler broadening or self-shielding. They didn't seem to realize that the energy dependent cross sections they produce in their evaluations are in the "cold", center-of-mass frame of reference, and this data can be factors of 100 (factors of 100 – not per=cent) different from what we use in our "hot", laboratory frame of reference calculations. I can only hope that one obvious purpose of this report is to make today's evaluators – and users – aware of these facts – facts, not fiction, since all of these effects can be experimentally measured using a combination of differential (energy dependent) and integral measurements.

Through VIII versions of ENDFB I have tried to accommodate changes introduced by physicists, some that were indeed BIG steps forward, such as adding the Reich-Moore resonance formalism, as well as those that I could see no good reason to include, since it was not obvious to me that a specific change was needed or indeed would in any was improve the data for use in our **Engineering applications**. But physicists insisted and CSEWG agreed to include these changes. Unfortunately, the changes in the latest ENDF/B-VIII.1, were beyond what I could approve of or even attempt to support in my PREPRO codes. After almost 60 years of my supporting ENDF using my PREPRO codes, the changes introduced in ENDF/B-VIII.1 crashed all of my codes. **This means my PREPRO codes that were never supported by any lab or institution are now dead,** and I have no intention of reviving them for general distribution. In the future I will continue to use them only for my own TART Monte Carlo applications. Fortunately, there are codes that are well financially supported and can carry on; in the U.S. this included AMPX (ORNL), and NJOY (LANL). So PREPRO is no longer needed as much as it has been in the past.

Here is a brief summary of the major ERRORS I see in today's ENDF/B-VIII.1,
1) ENDF-102 compliant cross sections can be defined by evaluators as the sum of up to three (3) terms: a) **Resolved** individual Resonances, b) Statistical representation of **Unresolved** Resonances, in MF=2; c) **tabulated cross sections** in MF=3. Today's evaluators do not seem to understand this division and/or definition of these three (3). The ENDF Resolved Region extends only up to the **LOWEST** energy where ALL L state resonances can be UNIQUELY defined. Today many ENDF/B evaluations extend their ENDF **Resolved** region well beyond this point up to where ALL L=0 state resolved resonances can be uniquely defined. This ignores the important narrow, unmeasurable L>0 resonances that cause Doppler broadening, leading to an incorrect Doppler effect, **important for Reactor Safety**. The ENDF **Unresolved** region does not uniquely define any energy dependent resonances or cross sections. It only defines the statistical distribution of resonances widths and spacings. This unresolved region allows for a smooth transition between the ENDF resolved region and a tabulated high energy region above the ENDF-102 Unresolved. Today's evaluators do not seem to realize that **any discontinuity in the total cross sections results in a non-physical discontinuity in the neutron flux calculated by our application codes**. What I see in many of today's evaluations beyond the ENDF Resolved, is no Unresolved; only about 20 % of ENDF/B-VIII.1 evaluations include an ENDF Unresolved region. In these cases, the Resolved is often followed by what appears to be experimentally measured resonances. This may look impressive on a plot, but it **does not meet our ENDF Engineering needs**. Being included above the Resolved region admits that this measured data is missing narrow Unresolved

resonances, which are so important in our Engineering applications. **Evaluators cannot simply dump measured data into the ENDF format and expect it to meet our Engineering needs.** I repeat, above the ENDF-102 Resolved there are no individual resonances; only an Unresolved statistical distribution, followed by a "smooth" tabulated high energy cross section.

2) Extending ENDF definitions to include more formalisms, such as Reich-Moore (R-M), was a BIG step forward for ENDF Cross Sections. But evaluators should be aware that the output from R-M codes, is in the **center-of-mass (C-M) system, "cold" (0 Kelvin).** Whereas in our applications we perform our calculations in the **Laboratory (LAB), with "hot" (e.g. 293.6 Kelvin; 20 Celsus)** Doppler broadened cross sections. By 1970 I had developed my SIGMA1 method to Doppler broadened ENDF MF=3 cross sections (the combinations of the 3 types described above), to create the "hot", LAB system cross sections we need in our applications. **But ENDF is designed for ONLY MF=3 cross sections to be temperature dependent**; my SIGMA1 method meets this need. But today's evaluators are misusing Reich-Moore code output of other data, such as neutron per fission, angular distributions (MF=4), energy distributions (MF=5), and others, "cold" data, in the **C-M system that is evaluated, "cold**". Evaluators should be aware that our processing codes have NO ability to handle any correlation to resonances to create temperature dependent data except for the MF=3 cross sections we need for use in our applications. 50 years ENDF evaluators and users knew we didn't need this correlation because the transformation from "cold", C-M, to "hot", LAB, makes this correlation disappear. My message to today's evaluators: use the standard codes we have successfully used for so many years to describe all secondary distribution's' i.e., everything except MF=3 cross section. Otherwise, what will be used in our applications is inconsistent "hot" MF=3 data, and "cold" secondary data, MF=4,5,…

3) Until ENDF was extend from 20 MeV to 100 MeV, there was no need for MT=5 (n, anything). When I first read this definition I thought it was a joke: "anything"; not a unique product as in the case of all other ENDF MTs. I was relieved when I read in ENDF-102 that **MT=5 was only to be used for complex reactions at high energy; I assumed above 20 MeV**. Unfortunately, today MT=5 is being misused, to define even simple reactions, like alpha production, all the way down to the ENDF lower energy limit of 10^{-5} eV. Our processing codes did not expect this, and I couldn't find any examples in ENDF/B-VIII.1 where it was needed. The worst example I found was in U235 where 80% of the lines of the evaluation were used to define alpha production, but nobody could uniquely define what the alpha production is; ENDF-102 says one thing and the evaluators says something else, because part of alpha production is hidden in MT=5. It really should not matter since however it is defined below the MeV energy range alpha production is 1,000,000 times less than the U235 total. Why this is included in this evaluation is beyond me; note, it was not included in earlier ENDF/B releases, and I couldn't find any applications where it is needed.

4) All the equations that use ATOMIC WEIGHT (ATWT) only apply to a specific atom – an ISOTOPE, not an ELEMENTAL mixture. You can get a very different answers if you scatter from a number of isotopes compared to scattering from an elemental mixture using its average atomic weight (ATWT). Similarly, you can get a different answer by first Doppler broadening ISOTOPES and then adding them together, compared to first adding them together and then Doppler

broadening; which would be incorrect. **ENDF should not include ELEMENTAL mixtures of ISOTOPES; only ISOTOPES.**

5) That is just the tip of the iceberg as far as what evaluators are doing WRONG today in ENDF/B evaluations; WRONG in the sense that it is counter to the purpose of ENDF-102 for use in **Engineering applications**. But I will stop here, because ALL of these ERROR have already been reported to NNDC and CSEWG as what I considered to be positive feedback that could be used to improve future versions of ENDF/B. But I was told that I was being negative and picking on CSEWG. So, I fear my attempt here will also fall on deaf ears; **There is none so blind as those that refuse to see.** But here goes my attempt to explain self-shielding to readers; this is another important effect that both evaluators and users should understand that makes what evaluators produce so much different from what neutrons "see" and interact with in our application codes.

Overview

In this paper I describe why Resonance Self-Shielding is so important, and I present examples to illustrate the magnitude of this effect. More importantly, in order to improve the accuracy of our results, I address what can be done to improve our treatment of self-shielding. Throughout I use recent ENDF data [1, 2], and Monte Carlo codes TART [3], and MCNP [4].

I point out the difference between Monte Carlo and deterministic codes (e.g., Sn), as it relates to how each treats self-shielding, particularly with regard to boundary conditions. Self-shielding means using energy averaged cross sections: obviously this applies to multi-group codes, but it also applies even to codes that use continuous energy cross sections [3, 4], to correctly include self-shielding in the unresolved resonance region [5, 6].

Lastly, I address the question of the statistical accuracy of Monte Carlo codes, and I present numerous examples, both very simple theoretical results, and hundreds of critical assemblies.

Please note that today our computers are fast enough and large enough that for my own applications with my TART Monte Carlo code [3], I always use continuous energy cross sections, not multi-group. Therefore, self-shielding is no longer a problem I must deal with, except in the unresolved resonance region [5, 6], where an "energy average" statistical approach is still required and used by both TART [3], and MCNP [4], see the appendix for details.

My conclusions include,

1) Failure to account for resonance self-shielding can give RUBBISH results. When you use unshielded cross sections be aware: **The results from any computer code can be no better than the data they use**; **with unshielded cross sections you can be in a: "garbage in = garbage out", situation.**
2) Standard methods of self-shielding in principle only apply to infinite, homogeneous media, but in practice they produce surprisingly accurate results for integral parameters, such as K_{eff}. However, they fail to accurately account for important spatial and directional results simultaneously for thick and thin media, such as spatially dependent fuel burn-up.

3) The multi-band method is designed to accurately reproduce both integral parameters, such as K_{eff}, as well as spatial and directional results, for media which are optically thick or thin media (multi-group does not) and generally multi-band results agree with results based on using continuous energy cross sections.

The multi-band method as used by TART [3] is used at all energies, whereas with MCNP [4] the Probability Table Method (PTM) has only been applied to self-shielding in the unresolved energy range. The multi-band method owes much to the earlier work of Nikolaev [23] and Levitt [24, 25]; it differs in providing an analytical solution to the multi-band equations, to explicitly conserve expected moments of the flux and reaction rates, and in using Monte Carlo [3], to make practical the correct, all important, boundary conditions, ala Nikolaev's all the way approach [23]. The results included in this report are based on using the multi-band method in the TART Monte Carlo code [3] for over 40 years, during which time it has been applied to thousands of applications.

The Multi-Group Problem

The problem with the Multi-Group method is that we have to "guess" the answer, in order to define the multi-group constants, and our "guess", even when using many groups (here I use 616 groups), can have a major impact on the accuracy of our answers.

Let's look at the source of the problem. The following applies to any geometry, but for simplicity, I will illustrate results starting from the time independent, linear transport equation, in planar geometry with continuous energy, and I will then explicitly describe the six models I used for the **continuous**, **multi-group** and **multi-band** cross sections,

$\mu\ \partial\Phi(E,z,\mu)/\partial z + \Sigma t(E,z)*\Phi(E,z,\mu) = R(E,z,\mu)$; here $R(E,z,\mu)$ is the slowing down and sources.

The multi-group equations are obtained by integrating over adjacent energy ranges, and usually spatial regions, and direction, to define multi-group constants,

$\mu\ \partial < \Phi(E,z,\mu)dE >/\partial z + <\Sigma t(E,z)*\Phi(E,z,\mu)dE> = <R(E,z,\mu)dE>$, or, equivalently,

$\mu\ \partial\Phi g(z,\mu)/\partial z + \Sigma tg(z)*\Phi g(z,\mu) = Rg(z,\mu)$

Where the group averaged total cross section is defined as **the group averaged ratio of reactions to flux,**

$$\Sigma tg(z) = \frac{<\Sigma t(E,z)*\Phi(E,z,\mu)dE>}{<\Phi(E,z,\mu)dE>} = \frac{\text{Reactions}}{\text{Flux}}$$

Our problem is that in order to define our multi-group cross sections, $\Sigma tg(z)$, we must "guess" at the **energy dependence** of the flux, $\Phi(E,z,\mu)$, which is the answer we are trying to find; sounds like a "Catch-22" situation. Less obvious we are integrating not only over energy, but usually **also over space and direction**. Generally, the energy dependent flux can be approximated by the product of two terms: **an energy dependent spectrum**, e.g., Maxwellian at low energy, 1/E in the slowing down range, and a fission and even possibly fusion source at higher energies, and **a cross section dependent,** self-shielding factor. For the slowing down spectrum here I assume it is

"smooth" in energy, which implies the **narrow resonance** (NR) approximation (an additional complication I will not address here). For a sufficiently large number of groups the assumption of the energy dependent term plays only a minor role, and since it appears in both numerator and denominator **its normalization plays no role at all**.

Unfortunately, the same cannot be said about the cross section dependent self-shielding factor. Here the effect is persistent for even many groups, indeed it plays a role as long as the width of a group is large compared to the width of resonances in the total cross section. We can see this by returning to our original energy dependent equation and assuming,

$\Phi(E,z,\mu) \sim \Phi(E,\mu)*Exp[K*z]$, similar to a Laplace transform or Case method

$$\{\mu K + \Sigma t(E,z)\}\Phi(E,\mu) = R(E,\mu)$$

$$\Phi(E,\mu) = \frac{R(E)}{\{\mu K + \Sigma t(E,z)\}}$$; here R(E) is an energy dependent term (no angular dependence); here the denominator is the self-shielding factor.

We can see here that neutron flux is inversely related to the total cross section, plus a spatially and direction dependent term, μK. One interpretation of the flux (the interpretation we use in our Monte Carlo codes) is that the flux is the distance travelled by the neutrons normalized per unit time, space, energy and direction; which helps us understand the above inverse relationship to the total cross section, e.g., doubling the total cross section will half the distance travelled by the neutrons, and hence result in half the flux. **This is referred to as "self-shielding" because it is the variation in the total cross section, itself, that causes variation in the flux;** it is this flux that we want to calculate using our multi-group equations, but as we can see here it is also the flux that we must "guess" in order to define our multi-group constants.

The most commonly used self-shielding models start from our above equation, and assume we have an **infinite, homogeneous** medium, i.e., ignore the μK term,

$$\Phi(E) = \frac{R(E)}{\{\Sigma t(E,z)\}}$$; note, here I have omitted the directional dependence of flux, $\Phi(E)$

An additional complication is that here the total cross section in the denominator is not the total of each evaluation (which is application independent), but rather it is the total of whatever mix of materials we are using in each spatial zone we are averaging over (obviously application dependent). Historically due to limited computer resources we wanted to only define application independent multi-group libraries, so another approximation is introduced; the **Bondarenko**, or partial shielding, where we assume that the total cross section for any mixture can be defined as that of each evaluation, plus a second cross section, Σ_0, which can be any value between zero (Totally Shielded) to infinity (Unshielded or infinitely dilute), cross sections,

$$\Sigma tg(z) = \frac{< \Sigma t(E,z)* R(E)\, dE/\{\Sigma t(E,z) + \Sigma_0\} dE>}{< R(E)\, dE/\{\Sigma t(E,z) + \Sigma_0\} dE>}$$; $\Sigma tg(z)$ constant within spatial zone (z)

Let's review the explicit approximations used to arrive at this equation,

1) Infinite, Homogeneous media; ignore μK.
2) Narrow resonances, which affects the slowing down spectrum, R(E).
3) Resonance structure in each evaluation independent; $\Sigma t(E,z) + \Sigma_0$

In addition, there are less obvious implied approximations.

1) Multi-group constants are constant throughout each spatial region
2) Multi-group constants are independent of direction

The below plots illustrate the ^{235}U and ^{238}U Total Cross Section using the TART 616 group structure (50 groups per energy decade from 10^{-5} eV to 20 MeV), comparing Unshielded and Totally Shielded cross sections. These plots illustrate that even with 616 groups, the ^{235}U Shielded Total can be up to ~ 75% less than the Unshielded (i.e.,1/4-th of it), and for ^{238}U it can be over 99% less (100 times less). **So the differences, even with 616 groups, due to self-shielding can be ENORMOUS; increasing to 2,020 groups does not improve things by much.**

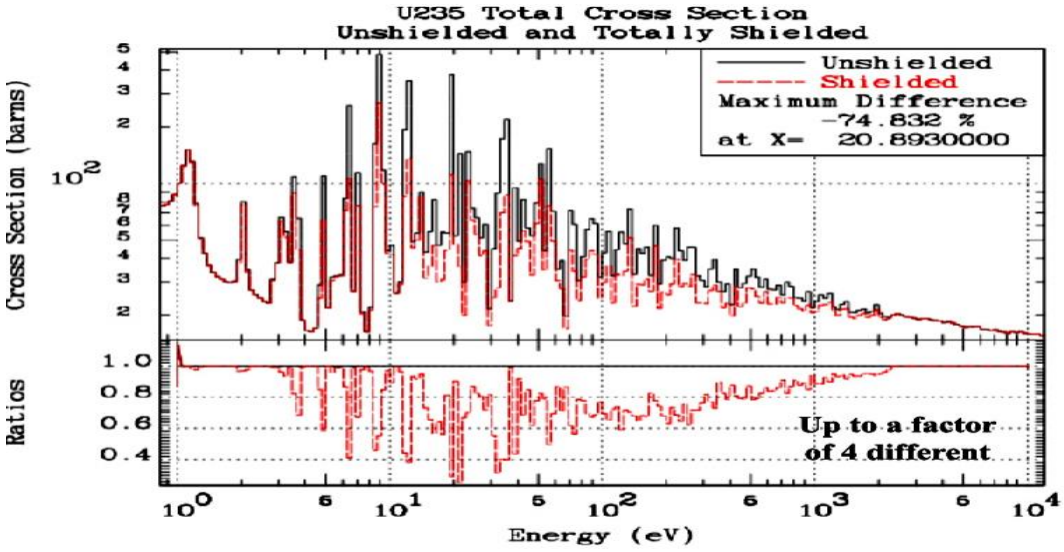

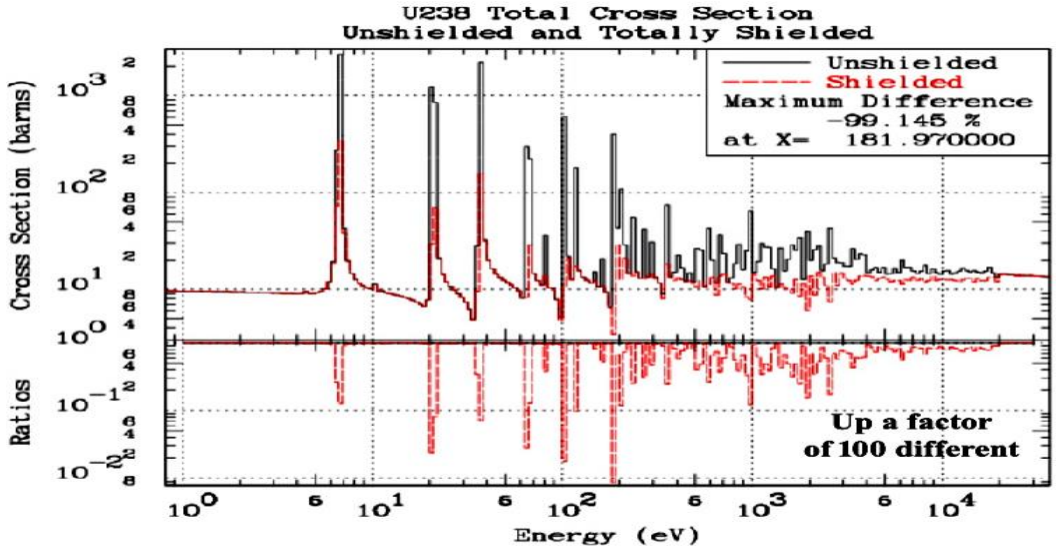

Spatial Zoning

One very important point to note: if a region of space contains only one mixture of materials, dividing this region into smaller and smaller volumes has no effect on these self-shielding models, so regardless of how fine we zone our geometry, this will not change the results shown below.

Cross Sections versus Distance of Collision

Note that above I only mention calculating the cross section, but in our Monte Carlo codes we sample the distance to collision, not the total cross section,

Distance = - log(random)/ $\Sigma t(E,z)$

Here we are trying to estimate the flux = the distance travelled by the neutrons. This suggests also that when we estimate the flux used as weighting in our multi-group equations, it should also be the distance to collision, or the inverse of the total cross sections, as shown in the above equations.

Six Cross Section Models

To illustrate the importance of self-shielding, I will use six different cross section models that I have included as options in the TART Monte Carlo code [3]. All the below differences shown for the simple 1-D planar, and 311 Slow Uranium problems are due solely to how these approximations are used in the six cross sections models; these six models include,

1) **Continuous** Energy Cross sections [7, 8], including Multi-Band shielding in the unresolved – this has the fewest approximations and here I assume produces the most accurate results to which all others are compared.
2) **Multi-Band** Cross Sections at ALL energies – uses the fewer approximations (as will be explained in detail below), and in this study it consistently produces results that agree closely with the Continuous energy results.
3) **Multi-Group** Cross Sections at ALL energies (unshielded energy averages) – this model completely ignores self-shielding and defines group averages by merely integrating over the energy range of each group,
   $\Phi(E,\mu) = R(E)$, completely ignoring the denominator, $\{\Sigma t(E,z) + \Sigma_0\}$.
4) **Unshielded Multi-Group** (defined from 2 Band Parameters, including unresolved) – this should be statistically equivalent to 3), but for this paper starts from 2 band parameters, and combines them to define unshielded cross sections.
5) **Totally** Shielded Multi-Group (defined from 2 Band Parameters, including unresolved) – this ignores the presence of any other materials in the mixture,
   $\Phi(E,\mu) = R(E,\mu) / \{\Sigma t(E,z)\}$, assuming $\langle\Sigma_0\rangle = 0$
6) **Partially** Shielded Multi-Group (defined from 2 Band Parameters), including unresolved) – uses the Bondarenko approximation, that each isotope in a material is independent,
   $\Phi(E,\mu) = R(E,\mu) / \{\Sigma t(E,z) + \langle\Sigma_0\rangle\}$
   Here I will note that this last "definition" is not necessarily unique, because a variety of multi-group processing codes treat $\langle\Sigma_0\rangle$ differently, e.g., is $\langle\Sigma_0\rangle$ the shielded or unshielded cross section for all other materials, and is it specific to each material included in each application? Accounting for the actual self-shielding in all other materials would require a multi-group processing code to iterate starting from an "application independent" multi-group data library. Here I use the unshielded cross section for each evaluation, in each group, to define $\langle\Sigma_0\rangle$ in all cases.

Definition of Criticality

Based on the literature you will find a number of different definitions of K_{eff},

1) A definition as the **eigenvalue of a mathematical problem**, to find the multiplier of fission nu-bar that will make a system self-sustaining. This can lead to a dangerously low estimate of K_{eff}, if there are any other processes, besides fission, that can contribute to neutrons. For example (n,2n) cannot by itself make a system critical, because there is no "upscatter". However, in the presence of fission, (n,2n) can contribute neutrons to an otherwise sub-critical system and make it critical.
2) A definition based on the **balance between neutron production and removal**; where removal includes both neutron absorption and leakage. Unlike definition 1), which only considers fission, this definition includes all neutron production, such as due to (n,2n), etc. For example, with a sub-critical assembly we can add a beryllium reflector, whose high (n,2n) can make the system critical. This is the definition used by the TART Monte Carlo code [3], and is the values presented in this paper.
3) A definition based on **Analog** Monte Carlo; for example, tracking neutrons collision by collision, and sampling one, and only one, outcome for each event (collision), only at the spatial point of the collision. This is a rather slowly converging process.
4) A definition based on **Expected** Monte Carlo; for example, rather than the Analog method, that only tallies one outcome per event, with Expected we tally continuously along the neutron track, based on ALL the cross sections that contribute to the total cross section. Compared to Analog, this converges more rapidly, particularly for integral parameters, such as K_{eff}. But in some cases, this can lead to loss of important correlations.

TART [3] always tallies both Analog and Expected results. This approach allows comparison of the two "answers" to check for convergence; in an unbiased sample we expect the two to converge to the same answer, as we sample progressively more neutrons. Generally, I quote Expected values in this paper, but I have also included some Analog results, which I have tried to clearly mark.

There are many well documented "critical" systems, for example TART [3] is distributed with over 1,000 "critical" systems [9], which are intended for testing purposes. But we must use caution, and carefully read the documentation for these systems, because not all are for actual critical systems (some are sub-critical), and all are simplified models (geometrically, and often materially). In addition, there is uncertainty in K_{eff} due to the nuclear data used; **the answer of any computer code cannot be any more accurate than the data it uses.** In this paper I assume the BEST, most physically acceptable, answer, will be that based on using the most detailed nuclear data, i.e., Continuous energy cross sections. WARNING: Due to the combination of many limitations, for any "approximate" model, the K_{eff} closest to unity, may not be the most "accurate"; again, a reminder that here I assume the answer based on using Continuous energy cross sections is the BEST, and I compare all other to this.

These limitations need not concern us in this paper, because rather than investigating how accurately we can produce K_{eff}, we will only be concerned with **how much K_{eff} is changed due to using one cross section model versus another: particularly, how resonance self-shielding affects K_{eff}.**

Simple, 1-D, Planar Example

To illustrate results I first calculated a very geometrically simple, theoretical critical system of a 1-D, planar, infinitely repeating array of Uranium layers in Water. I start with this extremely simple system to make it as easy as possible for anyone to replicate these results using other neutron transport codes, particularly deterministic codes.

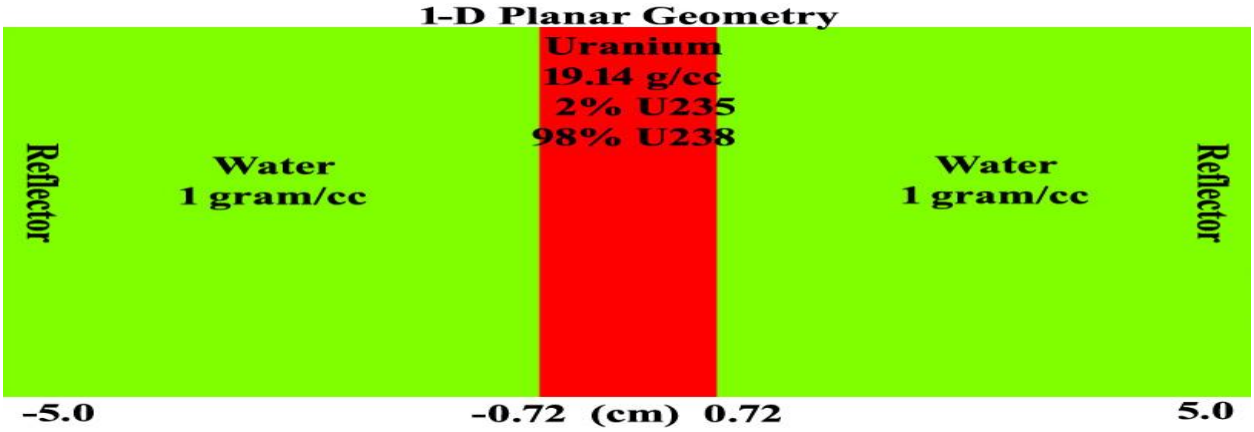

I used continuous energy cross sections as well as the TART 616 groups (50 per energy decade from 10^{-5} eV to 20 MeV) to represent the multi-group and multi-band cross sections (2 bands per group). The only difference in the calculations was the representation of the neutron cross sections as either continuous or multi-group (histograms), e.g., in all six cases I used the same continuous energy neutrons, geometry and reaction kinematics; only the multi-group (histogram), cross sections differed. Today we seem to have FAITH (faith = belief, without proof) that we can calculate K_{eff} to an accuracy of roughly 0.1% (3 digits), whereas the below results illustrate that if we do not account for self-shielding the difference between the results using continuous energy cross sections and 616 groups is over 0.025, 2.5%, or over 25 TIMES what we consider acceptable. Let me repeat what I wrote**: the difference is not 25%; it is 25 TIMES the 0.001 in K_{eff} 0.1%, that we consider acceptable. This difference is solely because of our "guess" for the flux that I used to define the multi-group constants, i.e., solely due to the self-shielding model.**

Note the running times: These are typical, showing that today using continuous energy cross sections is no longer prohibitively expensive, which is why **this is "The Standard BEST Option" that I use for all of my TART production work**; here I use multi-group and multi-band results solely in the hope that the results can be useful by others in their multi-group calculations; particularly deterministic calculations**.**

Planar U/Water Criticality Results

Cross Section Representation	Expected K-eff	Difference in K-eff	Removal Lifetime (Microsec.)	Median Energy (eV)	Seconds
Continuous	0.999924	--------	7.89162D+01	5.00948D-02	5066.660
Multi-Group	0.974683	-0.025241	7.70376D+01	5.01225D-02	3837.700
Multi-Band	1.000980	0.001056	7.90684D+01	5.01097D-02	4404.120
Unshielded	0.974645	-0.025279	7.70372D+01	5.01247D-02	4442.640
Totally Shielded	1.001750	0.001826	7.97356D+01	4.95769D-02	4581.800
Partial Shielded	0.991570	-0.008354	7.86170D+01	4.98773D-02	4512.280

Today we have FAITH (again, belief, without proof) that we can calculate critical systems within roughly 0.1%, i.e., 3-digits of accuracy. But the above results using 616 groups, demonstrates that,

1) Not self-shielding at all leads to differences of ~ 2.5%; **25 TIMES what we assume**.
2) Totally or Partially shielding improves results, but not to ~ 0.1%
3) Only the Multi-Band (in this case only 2 Bands) produces agreement ~ 0.1%.

I should stress that this is for a very simple, 1-D planar, system; far from what we expect to find in the real World.

Below is a picture of the neutron flux in the Uranium and Water, separately. The spectrum is more or less what we expect: a fission spectrum at high energy, a 1/E slowing down spectrum at intermediate energies, and a thermal Maxwellian. As it relates to this paper, note the minima in the flux in the Uranium near the peaks of the strongest ^{238}U resonances; exactly as predicted by Self-Shielding theory. Also, as we expect, there are no such minima in the water, showing the strong spatial dependence of the self-shielding.

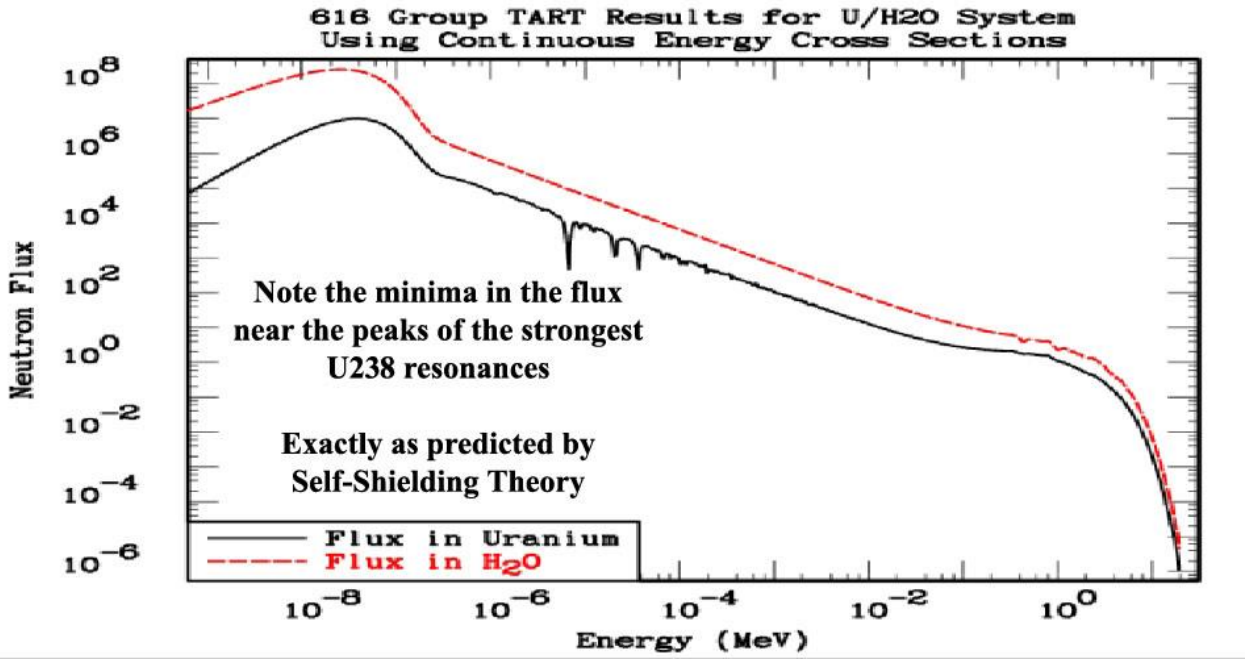

PLANE 1D: Reaction Details; based on one 10^{+8} neutron sample

The below tables present results using Continuous, Unshielded and Totally Shielded cross sections. Based on these tables it is easy for us to see the sources of the differences in K_{eff}; I have highlighted the important differences and similarities. Similarities include All predict about the same ^{238}U fast fission, and (n,2n) contributions (no self-shielding at high energy), as well as that most scatter is in the moderator (H_2O) , and there is no leakage from this theoretical, infinite 1D system. We see differences in elastic, capture, and fission, i.e., the resonance components.

PLANE 1D: Analog Events vs. Isotope per Removed Neutron

Continuous

Reaction	92235	92238	1001	8016
Elastic	0.04333	1.98132	50.68940	4.55955
(n,n')	0.00539	0.34429	0.00000	0.00092
(n,2n)	0.00002	0.00139	0.00000	0.00000
(n,3n)	0.00000	0.00001	0.00000	0.00000
Fission	0.37264	0.03073	0.00000	0.00000
(n,n'p)	0.00000	0.00000	0.00000	0.00000
(n,n'a)	0.00000	0.00000	0.00000	0.00001
(n,p)	0.00000	0.00000	0.00000	0.00001
(n,d)	0.00000	0.00000	0.00000	0.00000
(n,a)	0.00000	0.00000	0.00000	0.00242
(n,g)	0.06893	0.15345	0.37030	0.00011
Totals	0.49031	2.51118	51.05970	4.56301

Unshielded

Reaction	92235	92238	1001	8016
Elastic	0.04193	2.03861	49.64060	4.48570
(n,n')	0.00538	0.34454	0.00000	0.00092
(n,2n)	0.00002	0.00139	0.00000	0.00000
(n,3n)	0.00000	0.00001	0.00000	0.00000
Fission	0.36233	0.03078	0.00000	0.00000
(n,n'p)	0.00000	0.00000	0.00000	0.00000
(n,n'a)	0.00000	0.00000	0.00000	0.00001
(n,2a)	0.00000	0.00000	0.00000	0.00000
(n,p)	0.00000	0.00000	0.00000	0.00001
(n,d)	0.00000	0.00000	0.00000	0.00000
(n,a)	0.00000	0.00000	0.00000	0.00242
(n,g)	0.06699	0.17461	0.36134	0.00010
Totals	0.47666	2.58994	50.00190	4.48916

Totally Shielded

Reaction	92235	92238	1001	8016
Elastic	0.04369	1.97345	51.12700	4.58447
(n,n')	0.00538	0.34430	0.00000	0.00092
(n,2n)	0.00002	0.00138	0.00000	0.00000
(n,3n)	0.00000	0.00001	0.00000	0.00000
Fission	0.37346	0.03075	0.00000	0.00000
(n,n'p)	0.00000	0.00000	0.00000	0.00000
(n,n'a)	0.00000	0.00000	0.00000	0.00001
(n,p)	0.00000	0.00000	0.00000	0.00001
(n,d)	0.00000	0.00000	0.00000	0.00000
(n,a)	0.00000	0.00000	0.00000	0.00243
(n,g)	0.06705	0.15091	0.37387	0.00011
Totals	0.48960	2.50081	51.50090	4.58795

PLANE 1D: Analog Removal and Production per Removed Neutron.

The above table of results are **Expected,** and the below table are **Analog**; note the agreement in all cases to well within 3 digits (yet another indicator of convergence).

	Expected	Analog
Continuous	0.999924	0.999780
Unshielded	0.974645	0.974810
Totally Shielded	1.001750	1.001805

Continuous

Reaction	Removal	Production	Events
Elastic	0.000000	0.000000	57.273600
(n,n')	0.000000	0.000000	0.350596
(n,2n)	0.001412	0.002824	0.001412
(n,3n)	0.000008	0.000023	0.000008
Fission	0.403369	0.996932	0.403369
(n,n'p)	0.000000	0.000000	0.000000
(n,n'a)	0.000000	0.000000	0.000008
(n,p)	0.000007	0.000000	0.000007
(n,d)	0.000001	0.000000	0.000001
(n,a)	0.002419	0.000000	0.002419
(n,g)	0.592785	0.000000	0.592785
Leakage	0.000000	0.000000	0.000000
Totals	1.000000	0.999780	58.624200
K-eff		0.999779	

Unshielded

Reaction	Removal	Production	Events
Elastic	0.000000	0.000000	56.206800
(n,n')	0.000000	0.000000	0.350841
(n,2n)	0.001410	0.002820	0.001410
(n,3n)	0.000008	0.000024	0.000008
Fission	0.393117	0.971966	0.393117
(n,n'p)	0.000000	0.000000	0.000000
(n,n'a)	0.000000	0.000000	0.000007
(n,2a)	0.000000	0.000000	0.000000
(n,p)	0.000007	0.000000	0.000007
(n,d)	0.000001	0.000000	0.000001
(n,a)	0.002419	0.000000	0.002419
(n,g)	0.603039	0.000000	0.603039
Leakage	0.000000	0.000000	0.000000
Totals	1.000000	0.974810	57.557700
K-eff		0.974810	

Totally Shielded

Reaction	Removal	Production	Events
Elastic	0.000000	0.000000	57.728600
(n,n')	0.000000	0.000000	0.350606
(n,2n)	0.001402	0.002804	0.001402
(n,3n)	0.000008	0.000024	0.000008
Fission	0.404212	0.999007	0.404212
(n,n'p)	0.000000	0.000000	0.000000
(n,n'a)	0.000000	0.000000	0.000007
(n,p)	0.000007	0.000000	0.000007
(n,d)	0.000001	0.000000	0.000001
(n,a)	0.002434	0.000000	0.002434
(n,g)	0.591937	0.000000	0.591937
Leakage	0.000000	0.000000	0.000000
Totals	1.000000	1.001805	59.079200
K-eff		1.001805	

To better understand the source of these differences let us look inside the Uranium to see what is happening as far as the spatially dependent flux and the all-important reaction rates.

Flux, Reactions and Average Total Cross Section vs. Depth into Uranium

Our Monte Carlo codes track neutrons collision by collision as do discrete ordinate codes when they run analogue sweep by sweep. Let's look inside the Uranium to see the details of what happens for the first collision versus depth into the Uranium. We will be interested in the spatially dependent flux, reaction rates, and "local" average cross section (reaction/flux). I will use the Russian ABBN 26 group structure, which allows us to very clearly "see" self-shielding effects; these results will be similar to those seen using any group structure.

PLEASE understand that these are not Monte Carlo results; **they are analytical results** based on using a series of PREPRO [7] codes. The only uncertainty is that of the ENDF/B data [2]; there are no statistical uncertainties, as would occur with Monte Carlo or modelling errors as occur in either Monte Carlo or deterministic codes. Starting from ENDF/B cross section [8] the following series of PREPRO codes were used,

LINEAR/RECENT/SIGMA1: Linearly interpolable, tabulated, 293.6 Kelvin cross sections.
MIXER: Create the Uranium mixture: 2% ^{235}U, 98% ^{238}U.
GROUPIE: Calculate ABBN multi-group and multi-band cross sections.
VIRGIN: Calculate uncollided (i.e., virgin) flux, reaction rates, and cross sections.

With this approach the uncollided results are based on the actual Uranium mixture, of 2% ^{235}U and 98% ^{238}U, so that we avoid even the "partial" or Bondarenko approximation, i.e., for the multi-group results we need only consider **Unshielded** or **Totally** Shielded results. Anyone can re-create these, or any other, analytical uncollided results by FREELY downloading the ENDF data [8], and my PREPRO codes from my website [7].

The ABBN group structure uses three (3) groups per neutron energy decades; in any decade there are boundaries at 1, 2.15, 4.65, and 10 . Here I will show results only for one energy group from 100 to 215 eV (results in other groups are similar). To allow simple comparisons I will normalize the integral of the incident flux to be unity,

	Energy Dependent	Group Averaged
Flux	$\text{Exp}[-\Sigma t(E)*z/\mu]$	$\int_{E_g}^{E_{g+1}} \text{Exp}[-\Sigma t(E) * z/\mu]\, dE$
Reactions	$\Sigma t(E)*\text{Exp}[-\Sigma t(E)*z/\mu]$	$\int_{E_g}^{E_{g+1}} \Sigma t(E) * \text{Exp}[-\Sigma t(E) * z/\mu] dE$
Cross Section	Reactions/Flux = $\Sigma t(E)$	Reactions/Flux = **Variable in space**

The above results are general, since they apply to using either continuous energy or multi-group cross sections. It is informative to look at the special case where we are using multi-group cross sections, and the energy range that we use corresponds to only one group. Rather than a general energy dependent cross section we have, $\Sigma t(E) = <\Sigma t>$; the above general equations reduce to,

	Energy Dependent	Group Averaged
Flux	Exp[-<Σt>*z/ μ]	Exp[-<Σt>*z/ μ]
Reactions	<Σt>*Exp[-<Σt>*z/ μ]	<Σt>*Exp[-<Σt>*z/ μ]
Cross Section	Reactions/Flux = <Σt> = **Constant**	Reactions/Flux = <Σt> = **Constant**

First let's look at the actual energy dependent first collided total reaction rate versus depth into the Uranium, from a depth 0 to 0.72 cm (the midpoint of the Uranium, in the above simple problem), for the energy range 100 to 215 eV (one of the ABBN groups). This is followed by a detail of the 180 to 200 eV range, to more clearly see the results in one large resonance.

Note the reaction (Y axis) scale. By a depth of 0.72 cm there are virtually no remaining uncollided neutrons near the resonances and compared to the incident reaction rates at the surface (0 cm) the remaining reaction rates are up to 1,000 times lower, basically the only remaining reactions occur in the minima between resonances. From these figures even for very small depth (0.001 cm) we see significant self-shielding; even for as little as 0.0001 cm thickness the analytical calculations show significant reduction in the reaction rate (~ 20%).

What is important for the reader to understand is that in this case there is no reason for us to show the approximate energy dependent reaction used by the ABBN group structure, because by definition of "multi-group", it is constant across this entire energy range. After "seeing" the actual energy dependent reaction rate in the below figures you might question how accurate multi-group methods can be if they ignore this energy dependence. Multi-group results can be quite accurate, particularly to define simple integral parameters such as K_{eff}.

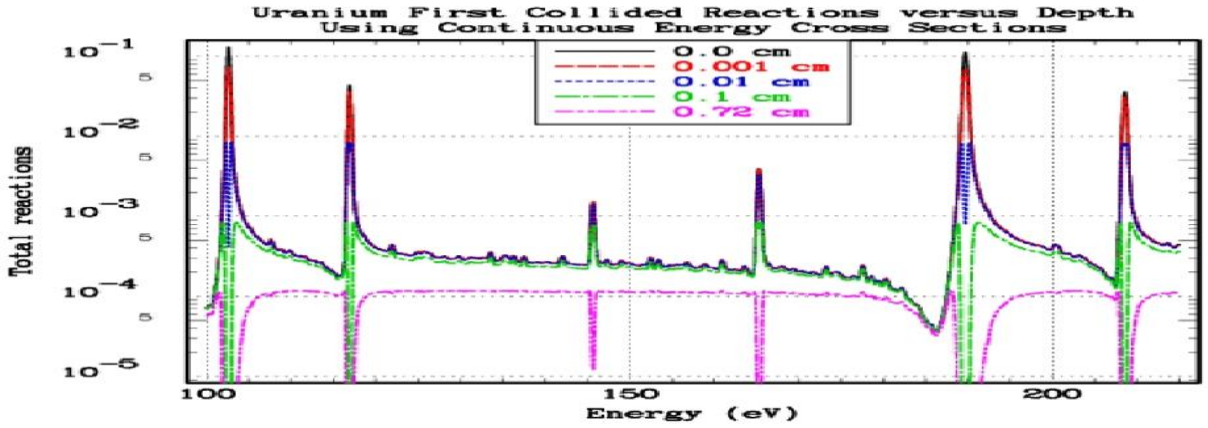

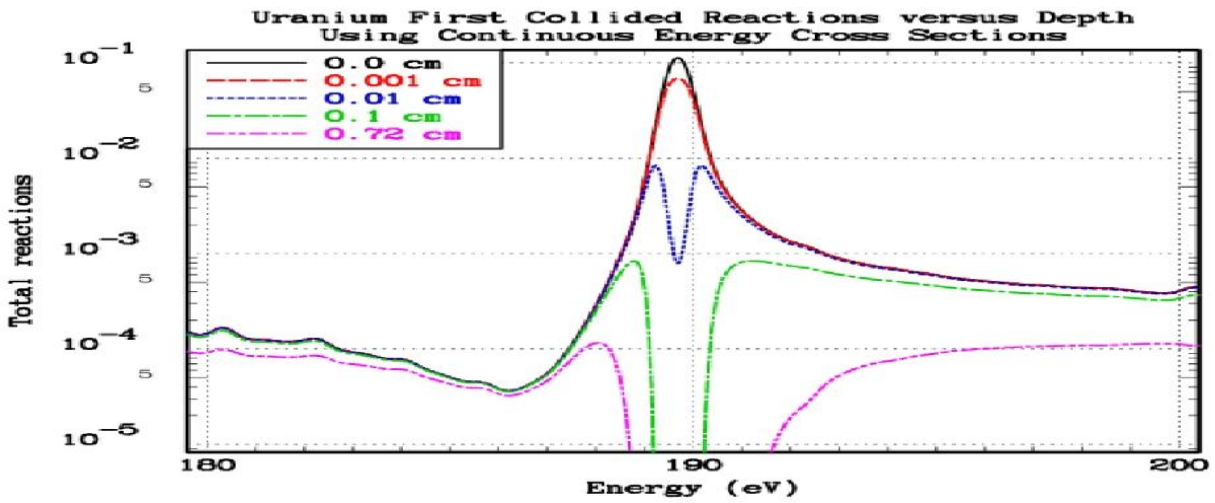

Next let's look at the group integrated results versus depth into the Uranium for the same single ABBN group from 100 to 215 eV. **Using continuous energy cross sections**, at the surface of the Uranium the neutrons have not yet "seen" the Uranium resonances, so strictly by cause and effect, we know there cannot be any self-shielding, i.e., **the correct "local" group averaged cross section MUST be the unshielded value**. As the neutrons progress further into the Uranium neutrons encounter the resonances, and within a very short distance the energy dependent flux nearest the resonances is heavily depressed (as we have seen in the above energy dependent figures), causing the "local" group averaged cross section (the ratio of group reactions to flux) to be dramatically self-shielded (as we have seen in the below spatially dependent figures). In the below figure we can see that the "local" group averaged average cross section decreases by about a factor of eight (8), from its highest, unshielded, value at the surface, to its heavily self-shielded value deep within the Uranium – **I repeat: a factor of 8!!!! Whereas all of our multi-group models assumes it is constant, independent of space within each zone; therein lies the problem with our multi-group models; they all suffer the loss of detail in space and direction.**

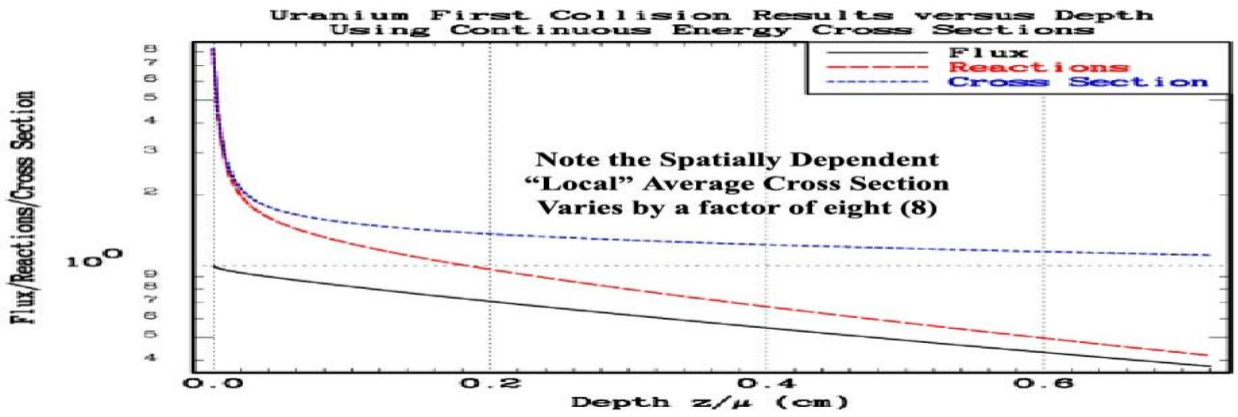

In contrast using **multi-group cross sections**, by definition, for each group the "local" average cross section is independent of depth, which means the flux and reaction rates within each group will show simple exponential attenuation into the Uranium. Using **Continuous Energy** or **Unshielded cross sections,** at the surface the "average" cross section is the same unshielded value, so the reaction rates are the same. However, with **Continuous** energy cross section the "local" cross section decreases with depth, allowing neutrons to penetrate further into the Uranium, making the reaction rate deep within the Uranium much higher than with unshielded multi-group cross sections; **in this case over a factor of more than a hundred (100) times higher**.

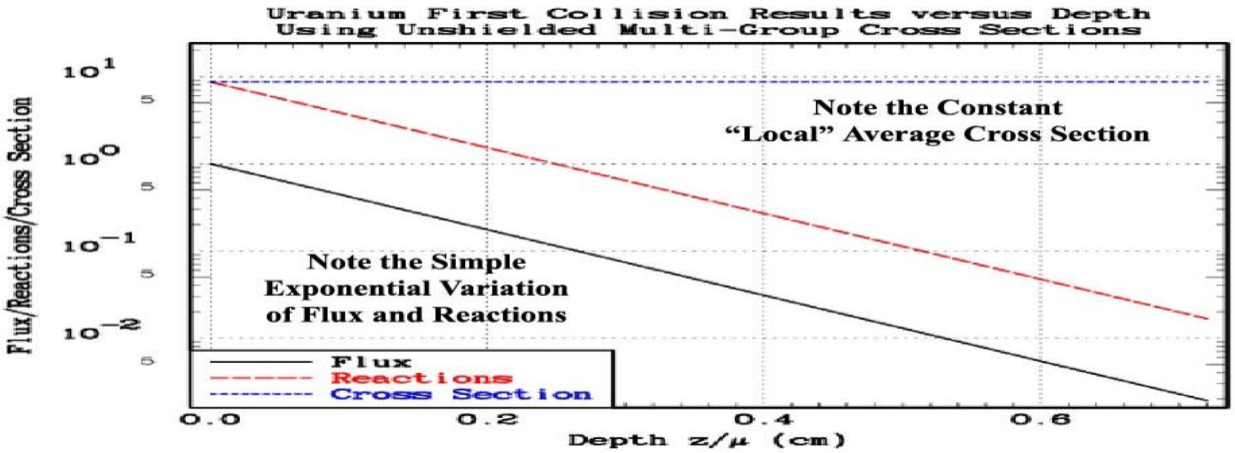

In the above figures the most obvious differences are because using continuous energy cross sections the "local" (z/ μ dependent) total cross section is variable, whereas with multi-group cross sections, by definition, the total cross section in any one group is a constant.

Next let's look at the same results using **Totally self-shielded** cross sections. Here the group averaged cross section is only about 1/8 that of the unshielded cross sections, so that the Uranium is optically thin and there is little attenuation. **Comparing these three figures, particularly the spatially dependent "local" average cross section using Continuous cross sections, to me it is amazing that the calculated K_{eff} only differ by a few per-cent.**

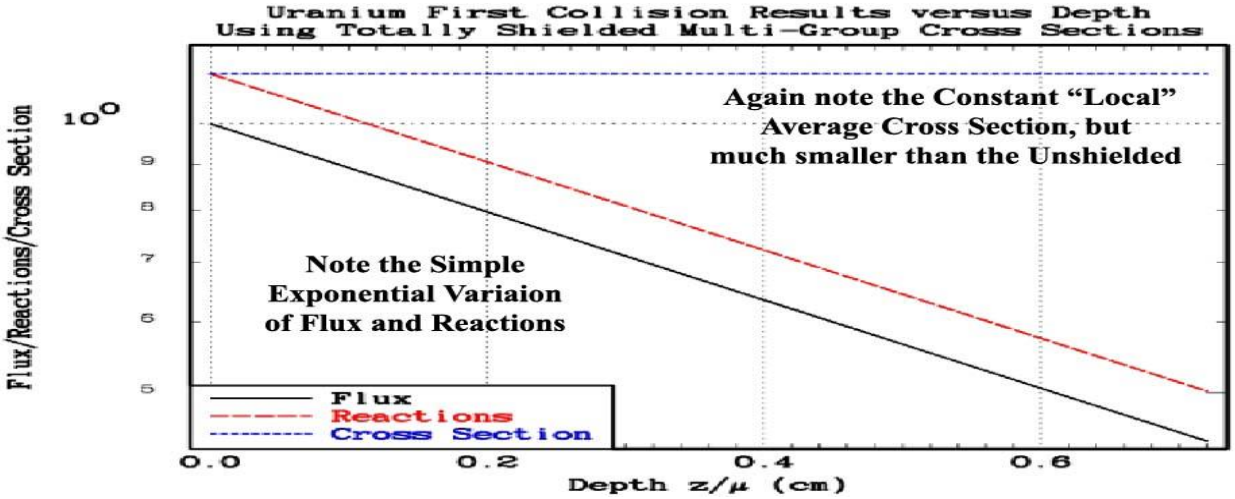

Below when we compare the **total reaction rates vs. depth** for these three cross sections models, we can see that the **Unshielded** model yields the same reaction rate at the surface but varies enormously everywhere else. Whereas **Totally shielding** yields much lower reaction rates near the surface (~ 8 times lower), but pretty good agreement deeper into the Uranium

.

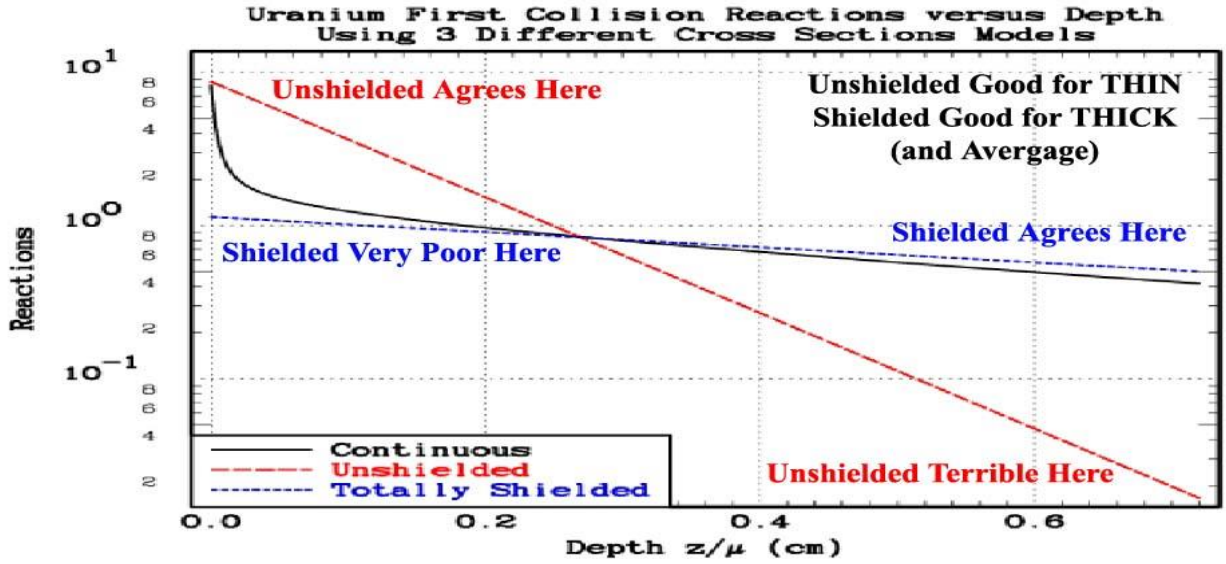

Through Thick or Thin: The above figure demonstrates that in order to **reproduce the spatially dependent Total Reactions** we need **Unshielde**d group averages for **THIN**, or small, depths (or thicknesses), and **Shielded** group averages for **THICK**, or larger, depths (or thicknesses) to reproduce spatial averages. **With only one degree of freedom (the group average) normal multi-group models cannot simultaneously satisfy both extremes**.

Below plotting the **Flux vs. Depth** clearly shows the problem with **Unshielded** cross sections, where it looks nothing like the **Continuous** cross section results; the Unshielded being up **to 200 TIMES less** than the Continuous results. The first below figure seems to show agreement between the **Continuous** and **Totally** Shielded results, however this is only because of the log Y scale. Switching to a linear Y scale, shows that in fact the **Totally** Shielded results are up to 30% greater than the **Continuous** results, and greater than the Continuous at all depths, so its integral will also be greater.

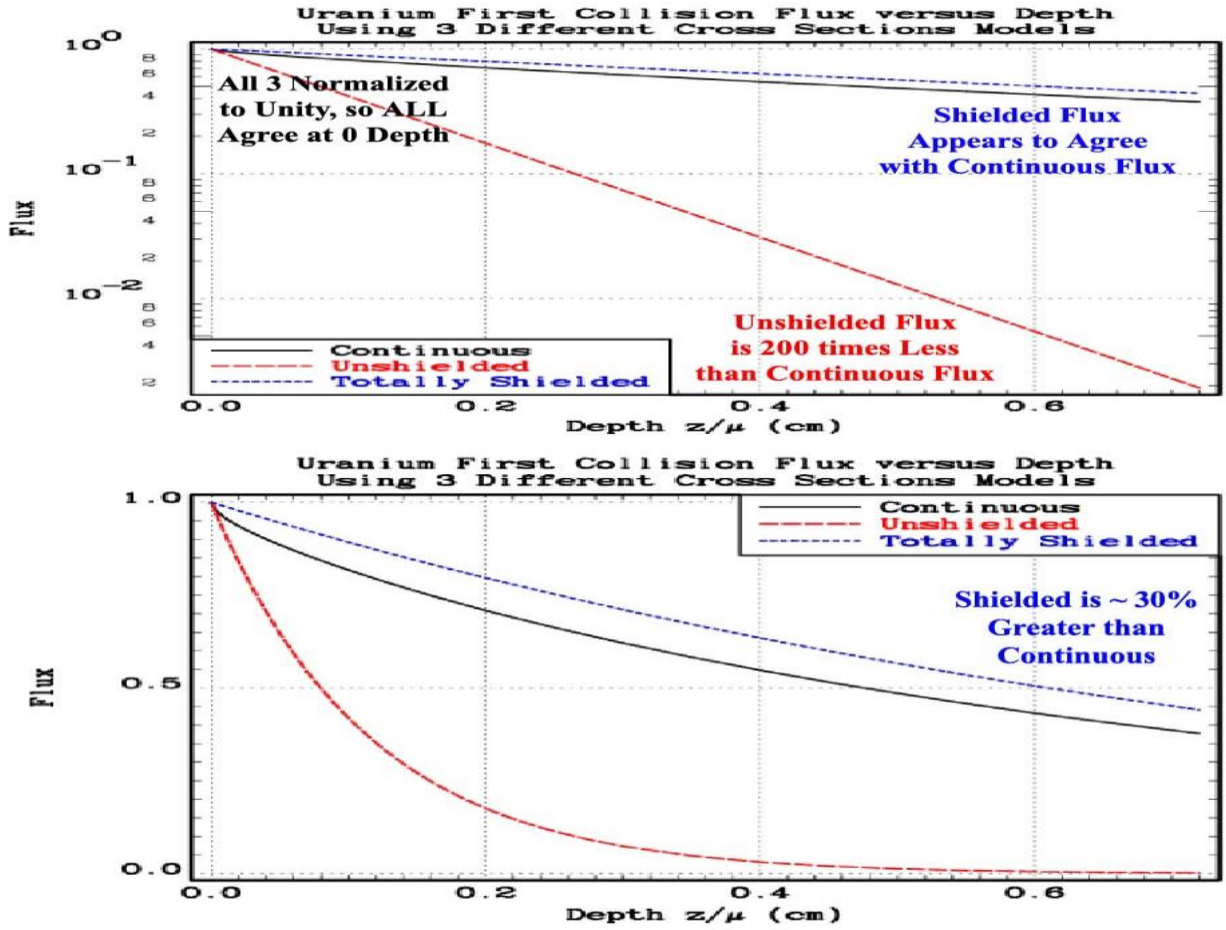

The above simple infinite repeat lattice is by far not the most difficult problem we will face; in general, K_{eff} = Production/[Absorption + Leakage], but our infinite system has no leakage, so that in this case K_{eff} is merely a ratio of reaction rates. Also, generally we will be interested in more than simple integral parameters, such as K_{eff}. For example, we may also be interested in the **spatially dependent burn-up**, which based on the above plots of **Continuous** reactions, will be high near the surface, as predicted by **Unshielded**, and nothing like the much lower reactions based on **Shielded** cross sections (~ 8 times too low).

Based of the above results, I will summarize the multi-group results by pointing out that in our neutron calculations in general we are interested in the scalar flux and current as well as reaction rate. The problem is that with only one degree of freedom (the multi-group cross sections), we cannot accurately simultaneously satisfy all these needs. Also as mentioned earlier, dividing into finer zones may not help, because using one of these multi-group self-shielding models, all zones may still have the same shielded cross sections.

The Multi-Band method [10, 11,12, 13, 14, 15], is designed to directly address these needs by introducing more degrees of freedom for each of the multi-groups. Physically we can think of each **energy group** divided into N **Total Cross Section Ranges** (Lebesque integration over cross section, instead of Riemann integration over energy). After our calculation we can add the N band results together to define the results for each group . Generally, using N cross section bands per group we have 2*N degrees of freedom; only 2*N – 1, because by definition of sum of the band weights MUST be unity. Here I will only use two (2) cross section bands, so we have four (4) constants that we can define for each group: P1, P2, Σ_{T1} ,Σ_{T2}. With this 2-band model the equivalent definitions of flux, reactions and "local" group averaged cross sections become,

	Group Averaged
Flux	$P1*Exp[-\Sigma_{T1}*z/\mu] + P2*Exp[-\Sigma_{T2}*z/\mu]$
Reactions	$\Sigma_{T1*}P1*Exp[-\Sigma_{T1}*z/\mu] + \Sigma_{T2*}P2*Exp[-\Sigma_{T2}*z/\mu]$
Cross Section	Reactions/Flux = **Variable**

Note, here we have two cross sections attenuating the neutrons, compared to only one for the multi-group model. I define these constants to ensure that in certain limiting cases we reproduce the known, or at least expected, limiting values, **basically the THIN and THICK limits** mentioned above,

1) P1 + P2 = 1 = normalization
2) The Unshielded value
3) The Totally Shielded value
4) One Partially shielded value, to follow expected $\Sigma 0 = 0$ to infinity self-shielding curve

These are four equations in four unknowns, so we expect a unique analytical solution to define four constants: P_1, P_2, Σ_{T1}, and Σ_{T2}. By inserting three weighting functions into our equation and equating the resulting equations to our **known, three pre-calculated self-shielded cross sections** [7, 16], $< \Sigma_0 >$, $< \Sigma_1 >$, $< \Sigma_2 >$ (Unshielded, Total, Partial),

$$1 = P_1 + P_2$$

$$\langle \Sigma_0 \rangle = \frac{\Sigma_{T1} P_1 + \Sigma_{T2} P_2}{P_1 + P_2} \quad ; \quad (W(\Sigma_T) = 1)$$

$$\langle \Sigma_1 \rangle = \frac{P_1 + P_2}{P_1 X_{T1} + P_2 X_{T2}} \quad ; \quad (W(\Sigma_T) = X_T) : \; X_T = 1/\Sigma_T$$

$$\langle \Sigma_2 \rangle = \frac{P_1 \Sigma_{T1} X^*_{T1} + P_2 \Sigma_{T2} X^*_{T2}}{P_1 X^*_{T1} + P_2 X^*_{T2}} \quad : \quad (W(\Sigma_T) = X^*_T) \; : X^*_T = 1/[\Sigma_T + \langle \Sigma_0 \rangle]$$

These are a set of non-linear equations; in this case with 2 bands, quadratic equations. We all know how to solve a quadratic equation [$x^2 + 2*b*x + c = 0$]; the solution is A+/-B, where: A = -b, and B = Sqrt[$b^2 - c$]; it's that simple. I used this to analytically define a unique solution to these four equations. We also know that there are similar solutions to cubic and quartic equations, so I also have analytical solutions for the 3 and 4 band equations, but in almost all cases 2 bands are more than adequate.

Making the standard change of variables used to solve a quadratic equation,

$$P_1 = \frac{1}{2} + \delta \quad ; \; \Sigma_{T1} = \frac{1}{X_1} = \frac{1}{A + B} \; ; \; P_2 = \frac{1}{2} - \delta \quad ; \; \Sigma_{T2} = \frac{1}{X_2} = \frac{1}{A - B}$$

This change of variables immediately satisfies $P_1 + P_2 = 1$ and the remaining three equations can be analytically solved to define,

$$A = \frac{1}{2 \langle \Sigma_1 \rangle} \left[\frac{\langle \Sigma_0 \rangle - \langle \Sigma_1 \rangle}{\langle \Sigma_0 \rangle - \langle \Sigma_2 \rangle} \right]$$

$$B^2 = \{ \langle \Sigma_1 \rangle A \left[\langle \Sigma_0 \rangle A - 2 \right] + 1 \} / [\langle \Sigma_0 \rangle \langle \Sigma_1 \rangle]$$

$$\delta = \frac{1 - A \langle \Sigma_1 \rangle}{2B \langle \Sigma_1 \rangle}$$

As expected, there are two possible values for B, corresponding to the positive and negative roots of B^2. This is the result of the non-uniqueness of the solution without an ordering. From the definitions of Σ_{T1}, Σ_{T2} and δ in terms of A and B, we can see that choosing the positive or negative root of B^2 merely corresponds to the same solution with the two bands interchanged. In order to obtain a unique solution, we will always define B to be positive, which corresponds to introducing the ordering $\Sigma_{T1} \le \Sigma_{T2}$.

The above algorithm will always produce physically acceptable parameters (positive band weights and cross sections) as long as $\langle \Sigma_0 \rangle \ge \langle \Sigma_2 \rangle \ge \langle \Sigma_1 \rangle$ (Unshielded ≥ Partial ≥ Total) . The only time that the three of these are equal is when the total cross section is independent of energy across the group (i.e., when it is constant); in all other cases this inequality is true. When the cross section is constant the two bands become indistinguishable and the two band cross sections become equal,

i.e., only one band is required in the group (i.e., the normal multigroup equation). WARNING – this is a limiting case that the codes GROUPIE [7], URRDO [5] and URRFIT [6], explicitly handle to avoid a singularity in the above definitions, as B and δ approach zero; this limit and how I handle it is described below.

In the seemingly trivial limit of no self-shielding, these equations become numerically unstable, because in this limit and two band cross sections, Σ_{T1} and Σ_{T2}, approach the unshielded average, and the two band weights, P_1 and P_1, become non-unique, as long as they sum to unity, e.g., we can see this from the equations defining B and δ, since in the no shielding limit B approaches zero and since δ is proportional to $1/B$, we have a problem.

To handle this limit, I consider three cases. In all three cases I always define,

$$P_1 = \frac{1}{2} + \delta \quad ; \Sigma_{T1} = \frac{1}{X_1} = \frac{1}{A+B} \quad ; P_2 = \frac{1}{2} - \delta \quad ; \Sigma_{T2} = \frac{1}{X_2} = \frac{1}{A-B}$$

The three cases correspond to placing limits on δ and/or B.

1) **No self-shielding**: $<\Sigma_1> = <\Sigma_0>$

Weight	$W(\Sigma_T) = 1$
Conserve	$<\Sigma_0>$

P1 = P2 = 1/2 : $\delta = 0$, $B^2 = 0$, $A = \mathbf{1}/<\Sigma_0>$

$\Sigma_{T1} = \Sigma_{T2} = <\Sigma_0>$

2) **Little self-shielding**: $<\Sigma_1> \Rightarrow 0.9999 <\Sigma_0>$; 0.01% or less self-shielding

Weight	$W(\Sigma_T) = 1$	$W(\Sigma_T) = 1/\Sigma_T$
Conserve	$<\Sigma_0>$	$<\Sigma_1>$

P1 = P2 = 1/2 : $\delta = 0$

$A = \mathbf{1}/<\Sigma_1>$

$B^2 = A^2 [<\Sigma_0> - <\Sigma_1>]/[<\Sigma_0>]$

3) **General self-shielding**: $<\Sigma_1> < 0.9999 <\Sigma_0>$; more than 0.01% self-shielding

Weight	$W(\Sigma_T)=1$	$W(\Sigma_T)=1/\Sigma_T$	$W(\Sigma_T)=1/(\Sigma_T + <\Sigma_0>)$
Conserve	$<\Sigma_0>$	$<\Sigma_1>$	$<\Sigma_2>$

$$A = \frac{1}{2<\Sigma_1>}\left[\frac{<\Sigma_0> - <\Sigma_1>}{<\Sigma_0> - <\Sigma_2>}\right]$$

$$B^2 = \{<\Sigma_1> A\ [<\Sigma_0> A - 2] + 1\}/[\ <\Sigma_0><\Sigma_1>]$$

$$\delta = \frac{1 - A<\Sigma_1>}{2B<\Sigma_1>}$$

Let's look at some results. The first plot below compares **FLUX**; here the **multi-band** results are similar, but somewhat better than the **shielded** results. Where we see the BIG difference is in the second plot below of **TOTAL REACTIONS**; here the multi-band results clearly outperform the shielded and unshielded results. The **multi-band** method reproduces the expected **unshielded** results at the surface (depth = 0), where the **shielded** results are far too low (in this case a factor of ~ 8 too low). The **multi-band** method also reproduces the expected **shielded** results at large depths, where the **unshielded** results are very poor. And most important, across the entire depth range **the multi-band results are in closer agreement with the real Continuous results versus depth, so its integral will be closer, which is what we are interested in to accurately calculate K_{eff}.**

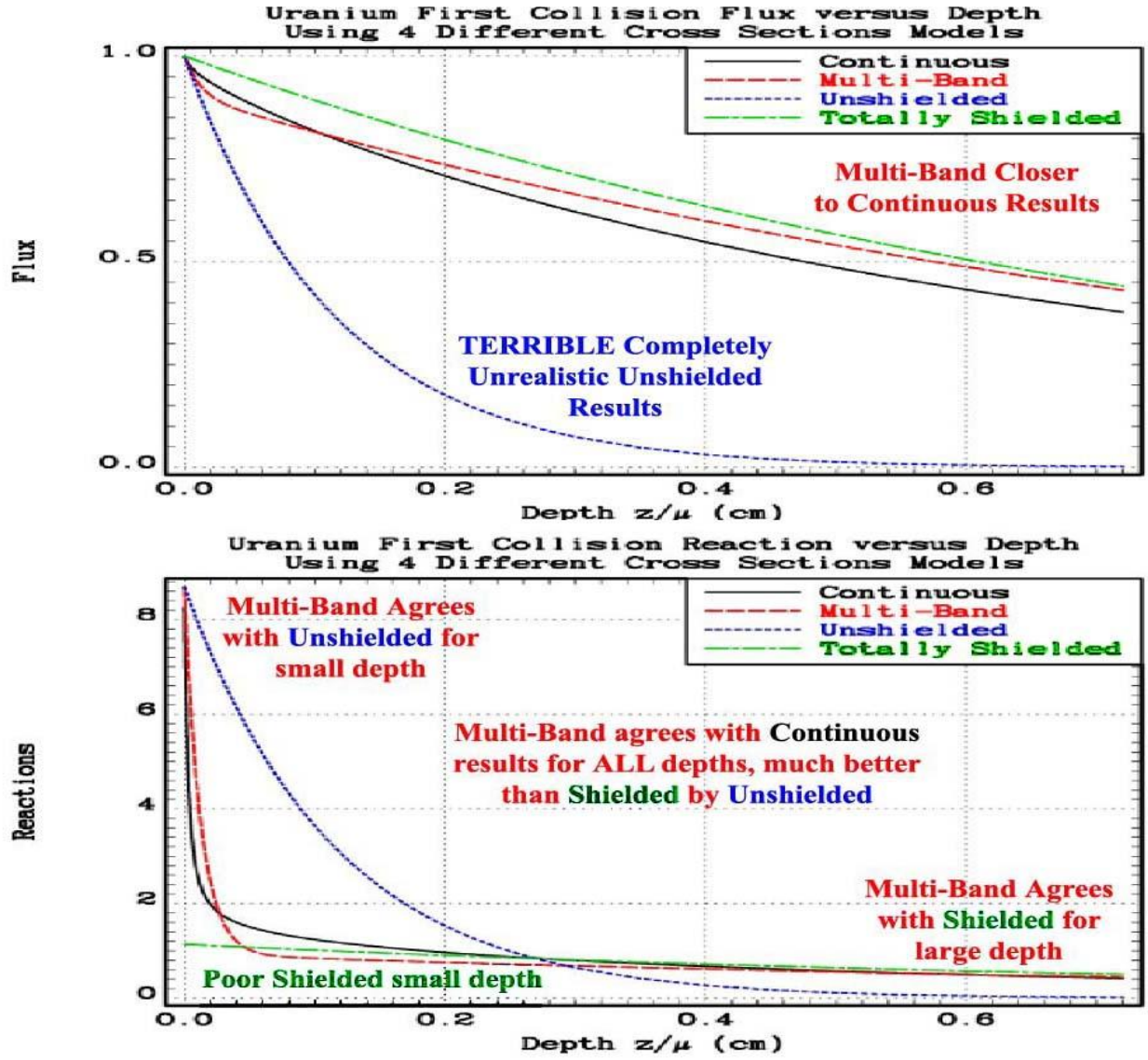

Usually when one thinks of multi-group data, one only considers an "average" over energy, but in fact **the "average" is really over (energy, space, direction**). Hopefully the above results clearly show the need for improved spatial results, which the multi-band method is designed to provide. Less obvious is that the **multi-band method also improves directional results**. For example, at the surface of the fuel the multli-band method is designed to reproduce the **unshielded incident** fux and reaction rate (as shown above). But it will also reproduce the **shielded leakage** from the surface of the fuel. In other words: **at exactly the same spatial point (the surface) the multi-band method can reproduce the angular incident and reflected flux and reaction rates**; something multi-group "averages" cannot do. This is equivalent in a discrete ordinate code having different " group average" cross sections in each discrete direction, which the 2 multi-band cross sections combine to reproduce.

Transmission Measurements

The above results for the Uncollided flux and Reaction Rates are more than an Academic Exercise that we can never actually observe. They correspond to the measurement of well columnated transmission through a range of thicknesses for any given material; in the above case the transmission through a material composed of 2% ^{235}U and 98% ^{238}U. In these measurements, "**self-indication**" corresponds to measuring **reaction rates** and "**flux**" obviously corresponds to the **flux** shown above.

There are many such measurements and reports analyzing these measurements. As it relates to this paper, I will mention the measurements of Bramblett and Czirr for ^{239}Pu [17] and ^{235}U [18], who reported results for transmission measurements through ^{239}Pu and ^{235}U, integrated over a series the ABBN groups, i.e., the same quantities as shown above, but for different materials. These measurements have been extensively analyzed to show the same self-shielding effects [19, 20, 21] as seen in the above figures, so I will not repeat these calculations here. I will merely state that these earlier measurements and calculations verify the self-shielding results shown above, i.e. **these results are real and important to include in multi-group calculations if we expect to produce accurate results, particularly all-important reaction rates.**

It would be wonderful to have a similar self-indication measurement for ^{238}U (hint, for any experimentalists who may be reading this). This would be a very difficult measurement due to the very narrow ^{238}U resonances. The above results indicate that this measurement would require extremely thin foils; the above analytical calculations show that a thickness of only 0.0001 cm (that is not a typo, 10^{-4} cm) reduces the total reaction rate by ~ 20%. By a thickness of only 0.1 cm almost all the self-shielding due to ^{238}U resonance is complete; there are but few neutrons remaining in the energy range of major resonances; see the above plot of the energy dependent spectra versus energy and depth.

Statistics

Unfortunately, too many people assume that since they are using Monte Carlo with continuous energy cross sections this will result in the BEST possible answer. However, anytime we use Monte Carlo we must be sure to run enough samples to ensure convergence, this is particularly true when using continuous energy cross sections. When using **multi-group** cross sections our Monte Carlo codes need only sample a limited number of cross section values. In contrast with **continuous energy cross sections** the code must sample many thousands of tabulated values, as well as the interpolated values between tabulated values. This can require a very large number of samples to TRULY achieve convergence to a final answer.

For the results shown in this report for each of six different cross section models I used 100 million (10^{+8}) neutron samples, for each of 311 ^{235}U slow critical systems [22], i.e., 6 Models X 10^{+8} samples X 311 assemblies ~ $2*10^{+11}$ neutron samples. In my home, on my DELL desktop with 6 processors and 24 GB memory, running all six cross section models simultaneously, this took roughly a week. Was this much time necessary? Yes, if we really want to ensure the differences I present here have truly converged to the accuracy that we claim today. Today many users have FAITH (again, faith = belief, without proof) that we can calculate Monte Carlo criticality K_{eff} results to ~ 0.1% accuracy (3 digits). Generally, Monte Carlo will converge to one stable final answer with an uncertainty of R/Sqrt(S), where R is a system dependent constant, and S is the number of independent samples used, e.g., **reducing the uncertainty by a factor of 10 requires roughly 100 times as many samples.**

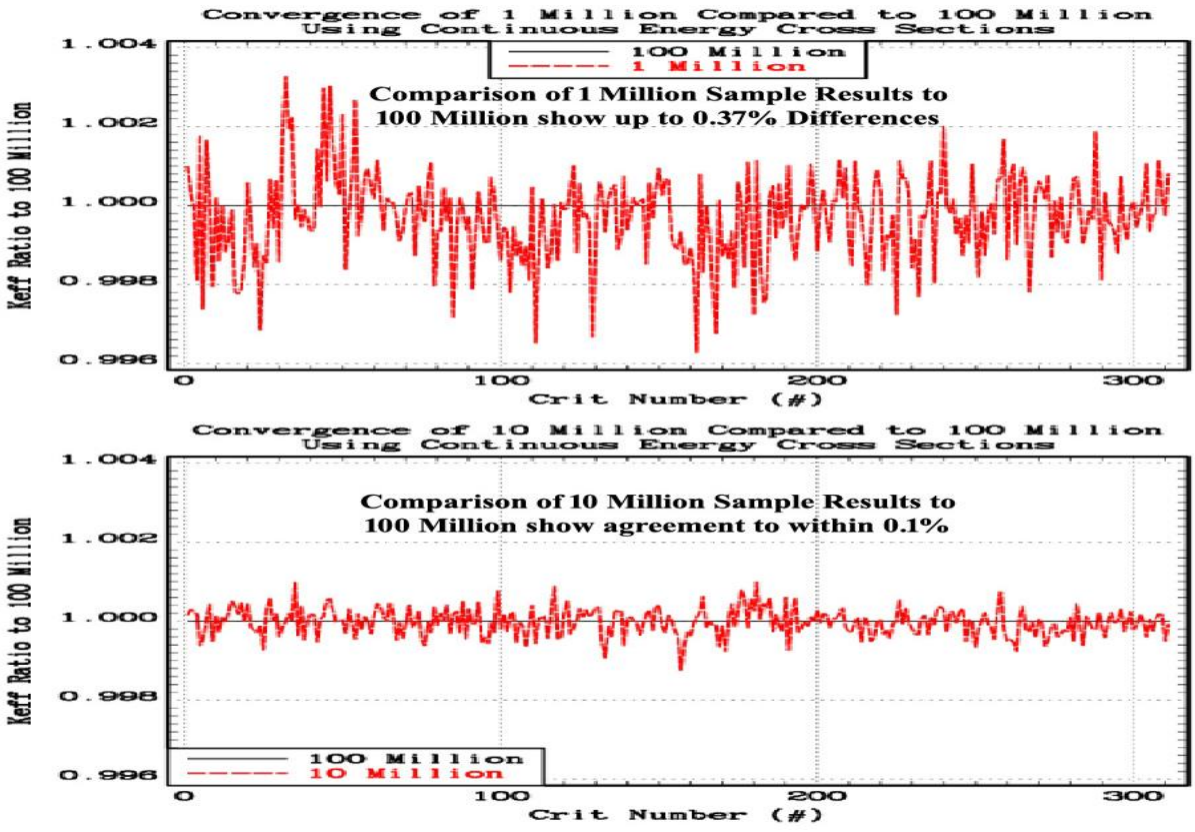

Here to illustrate convergence I used **Continuous** energy cross sections to compare results for 311 ^{235}U slow critical assemblies [8] for: 10^{+6} ,10^{+7}, 10^{+8}, and neutron samples. The above figures show that 10^{+6} results differ from the 10^{+8} results by up to 0.37%, and 10^{+7} results have converged to within 0.1% of the 10^{+8} .

Note the 1/Sqrt(S) convergence: 10^{+6} 0.37%, 10^{+7} 0.1%, and a assume (have faith) that the 10^{+8} results are ~ .03%, well within the accuracy we need for this study. Hopefully this explains why I used at least 10^{+8} samples for ALL of the final results = it is necessary to validate the accuracy that I claim.

WARNING: Hopefully these results demonstrate that when comparing differences, as in this study, users must not be in a rush to finish calculations by using too few samples. If you use too few your answers – and conclusions – can be incorrect, and rather than saving time you will end up wasting it. PLEASE remember Howerton's First Law: **We are in NO rush for the WRONG answer.**

311 U-235 Slow Critical Assemblies

In an earlier report I published results of K_{eff} calculated by TART [3] for 1,172 Critical Assemblies [22], so this has already been done, and need not be repeated here. Here my focus is not on the BEST calculated K_{eff}, but rather on the difference between the BEST calculated K_{eff}, using **Continuous** energy cross sections, and the five (5) **multi-group** and **multi-band** models discussed here. In order to demonstrate these differences, I used all 311 ^{235}U Slow Assemblies for my earlier report [22]. From the first figure below, we can see that rather than achieving agreement to 0.1% (3 digits), **I found differences up to almost 9% for the multi-group unshielded and shielded models**. In contrast the second figure shows close agreement using 2 Bands, but even it has some problems with assemblies 207 through 231 (LCT006, LMT001, LMT002). In this report I only present 2 bands Narrow Resonance (NR) results, comparable to what other multi-band codes can calculate; see, the appendix for Intermediate Resonance (IR) TART [3] results for assemblies 207 through 231. **Of the models discussed here the multi-band clearly out performs the four strictly multi-group models.**

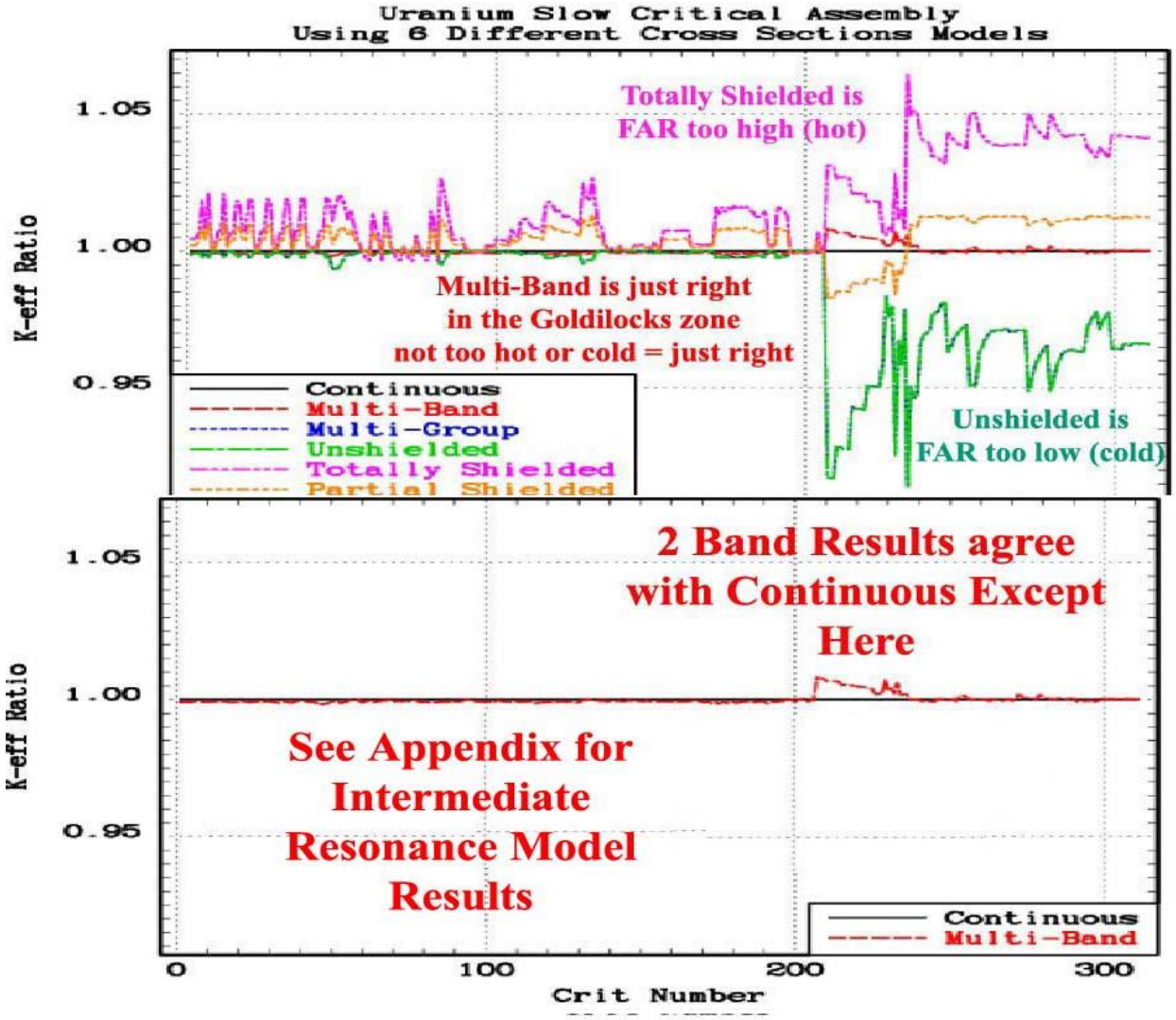

LCT006-1: Reaction Details; based on one 10^{+8} neutron sample

The below tables present results using Continuous, Unshielded and Totally Shielded cross sections. Based on these tables it is easy for us to see the sources of the differences in K_{eff}; I have highlighted the important differences and similarities. Similarities include: All predict the same ^{238}U fast fission, and (n,2n) contributions (no self-shielding at high energy), as well as that most scatter is in the moderator (H_2O) (large n,n' is due to bound H) , and small leakage from the system. We see differences in: elastic, capture, and fission, i.e., the resonance components.

LCT006-1: Analog Events vs. Isotope per Removed Neutron

Continuous

Reaction	92238	92235	8016	92234	13027	1001	7014
Elastic	1.88951	0.05271	5.70417	0.00064	0.38601	11.79320	0.00017
(n,n')	0.24331	0.00502	0.00136	0.00002	0.01297	51.41410	0.00000
(n,2n)	0.00091	0.00002	0.00000	0.00000	0.00000	0.00000	0.00000
(n,3n)	0.00000	0.00000	0.00000	0.00000	0.00000	0.00000	0.00000
Fission	0.02204	0.38300	0.00000	0.00003	0.00000	0.00000	0.00000
(n,n'p)	0.00000	0.00000	0.00000	0.00000	0.00002	0.00000	0.00000
(n,n'a)	0.00000	0.00000	0.00001	0.00000	0.00000	0.00000	0.00000
(n,p)	0.00000	0.00000	0.00001	0.00000	0.00018	0.00000	0.00001
(n,d)	0.00000	0.00000	0.00000	0.00000	0.00000	0.00000	0.00000
(n,t)	0.00000	0.00000	0.00000	0.00000	0.00000	0.00000	0.00000
(n,a)	0.00000	0.00000	0.00386	0.00000	0.00003	0.00000	0.00000
(n,g)	0.18303	0.07714	0.00010	0.00140	0.00482	0.30584	0.00000
Totals	2.33881	0.51789	5.70951	0.00210	0.40403	63.51310	0.00018

Unshielded

Reaction	92238	92235	8016	92234	13027	1001	7014
Elastic	1.98423	0.04979	5.55550	0.00059	0.37873	11.53880	0.00016
(n,n')	0.24260	0.00501	0.00136	0.00002	0.01294	50.15130	0.00000
(n,2n)	0.00091	0.00002	0.00000	0.00000	0.00000	0.00000	0.00000
(n,3n)	0.00000	0.00000	0.00000	0.00000	0.00000	0.00000	0.00000
Fission	0.02201	0.34938	0.00000	0.00003	0.00000	0.00000	0.00000
(n,n'p)	0.00000	0.00000	0.00000	0.00000	0.00002	0.00000	0.00000
(n,n'a)	0.00000	0.00000	0.00001	0.00000	0.00000	0.00000	0.00000
(n,p)	0.00000	0.00000	0.00001	0.00000	0.00017	0.00000	0.00001
(n,d)	0.00000	0.00000	0.00000	0.00000	0.00000	0.00000	0.00000
(n,t)	0.00000	0.00000	0.00000	0.00000	0.00000	0.00000	0.00000
(n,a)	0.00000	0.00000	0.00386	0.00000	0.00003	0.00000	0.00000
(n,g)	0.23168	0.07023	0.00009	0.00128	0.00441	0.29873	0.00000
Totals	2.48143	0.47443	5.56083	0.00192	0.39631	61.98880	0.00017

Totally Shielded

Reaction	92238	92235	8016	92234	13027	1001	7014
Elastic	1.85213	0.05411	5.79611	0.00054	0.38256	11.93760	0.00018
(n,n')	0.24381	0.00505	0.00136	0.00003	0.01300	52.39080	0.00000
(n,2n)	0.00092	0.00002	0.00000	0.00000	0.00000	0.00000	0.00000
(n,3n)	0.00000	0.00000	0.00000	0.00000	0.00000	0.00000	0.00000
Fission	0.02211	0.39577	0.00000	0.00003	0.00000	0.00000	0.00000
(n,n'p)	0.00000	0.00000	0.00000	0.00000	0.00002	0.00000	0.00000
(n,n'a)	0.00000	0.00000	0.00001	0.00000	0.00000	0.00000	0.00000
(n,p)	0.00000	0.00000	0.00001	0.00000	0.00018	0.00000	0.00001
(n,d)	0.00000	0.00000	0.00000	0.00000	0.00000	0.00000	0.00000
(n,t)	0.00000	0.00000	0.00000	0.00000	0.00000	0.00000	0.00000
(n,a)	0.00000	0.00000	0.00389	0.00000	0.00003	0.00000	0.00000
(n,g)	0.16668	0.07495	0.00010	0.00102	0.00507	0.31130	0.00000
Totals	2.28565	0.52990	5.80148	0.00162	0.40086	64.63970	0.00018

LCT006-1: Analog Removal and Production per Removed Neutron

Continuous

Reaction	Removal	Production	Events
Elastic	0.000000	0.000000	19.826400
(n,n')	0.000000	0.000000	51.676700
(n,2n)	0.000931	0.001863	0.000931
(n,3n)	0.000005	0.000014	0.000005
Fission	0.405076	0.997110	0.405076
(n,n'p)	0.000000	0.000000	0.000017
(n,n'a)	0.000000	0.000000	0.000010
(n,p)	0.000191	0.000000	0.000191
(n,d)	0.000001	0.000000	0.000001
(n,t)	0.000000	0.000000	0.000000
(n,a)	0.003894	0.000000	0.003894
(n,g)	0.572330	0.000000	0.572330
Leakage	0.017571	0.000000	0.000000
Totals	1.000000	0.998987	72.485600
K-eff		0.998986	

Unshielded

Reaction	Removal	Production	Events
Elastic	0.000000	0.000000	19.507800
(n,n')	0.000000	0.000000	50.413200
(n,2n)	0.000933	0.001865	0.000933
(n,3n)	0.000005	0.000014	0.000005
Fission	0.371423	0.915064	0.371423
(n,n'p)	0.000000	0.000000	0.000018
(n,n'a)	0.000000	0.000000	0.000011
(n,p)	0.000189	0.000000	0.000189
(n,d)	0.000002	0.000000	0.000002
(n,t)	0.000000	0.000000	0.000000
(n,a)	0.003895	0.000000	0.003895
(n,g)	0.606421	0.000000	0.606421
Leakage	0.017133	0.000000	0.000000
Totals	1.000000	0.916944	70.903900
K-eff		0.916943	

Totally Shielded

Reaction	Removal	Production	Events
Elastic	0.000000	0.000000	20.023300
(n,n')	0.000000	0.000000	52.654000
(n,2n)	0.000938	0.001877	0.000938
(n,3n)	0.000005	0.000015	0.000005
Fission	0.417913	1.028410	0.417913
(n,n'p)	0.000000	0.000000	0.000018
(n,n'a)	0.000000	0.000000	0.000011
(n,p)	0.000197	0.000000	0.000197
(n,d)	0.000001	0.000000	0.000001
(n,t)	0.000000	0.000000	0.000000
(n,a)	0.003925	0.000000	0.003925
(n,g)	0.559116	0.000000	0.559116
Leakage	0.017906	0.000000	0.000000
Totals	1.000000	1.030300	73.659400
K-eff		1.030300	

Is it the model or Statistics?

Before jumping to any conclusions let's take a closer look at these 311 ^{235}U slow critical assemblies. Most of these are geometrically simple large assemblies, that's why we see better agreement for the first 200 or so. But starting with # 207, LCT006-1, there are a series of geometrically complicated assemblies. Below is a TARTCHEK [3] view of LCT006-2 which shows an array of 20 x 20 = 400 fuel pins in a roughly 43 x 43 cm space. Remember, that all four of the Multi-Group models used here assume an **infinite, homogenous** medium (they ignore μK; directional and spatial streaming). In the LCT006 series there are rather strong neutron currents flowing in and out of each fuel pin, so we would expect differences when we use cross sections designed for infinite, homogeneous models.

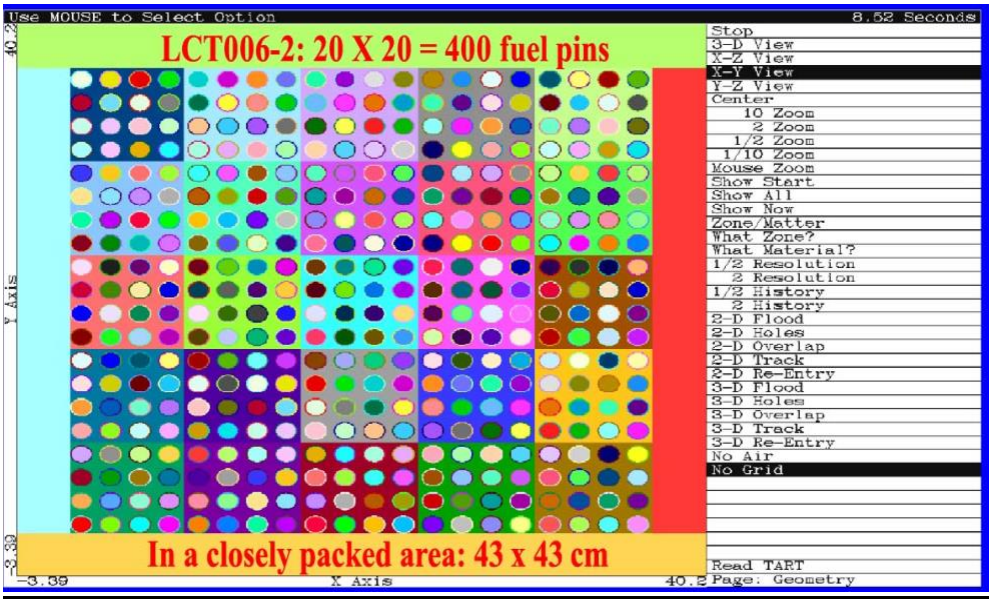

Mark Twain said, "There are LIES, DAMN LIES, and STATISTICS". Here I want to be sure we answer the question: **Are the above differences due to the cross section model or statistics?** Even using 10^{+8} active neutrons to calculate each assembly, one might question whether this is sufficient to guarantee convergence, for the LCT006 series, e.g.., for each of the 400 fuel pins we are only sampling 10^{+8}/400 pins = 250,000 neutrons/pin.

In order to test the accuracy of the above results, I re-ran one of the most complicated assemblies, LCT006-1, which is a 19 X 19 array, similar to the one shown above. I used the TART input option to re-run LCT006-1 100 times, using all six cross section models. To start I ran TART using 1,000 settle cycles (to minimize the effect of the initial flux guess), followed by 10^{+7} active neutrons for each of 100 statistically independent calculations using different random number sequences; this is a cumulative sample of 10^{+9} source neutrons for each of the six cross section models. The below results are absolute K_{eff} results, not ratios to the Continuous results. For each model the below tables define:

1) The Average and standard deviation, as well as Lowest and Highest of the 10^{+7} 100 results
2) A comparison to a Normal Probability Distribution, as far as the expected distribution of results relative to the average and using the standard deviation.

By 10^{+9} samples the standard deviation of all six models, are well below the 0.1% level. For each model the spread in results and comparison to a Normal Distribution show that even by 10^{+7}, there are no abnormal results beyond +/- 4 standard deviations. **In other words: Statistically this is about as good as it gets. These results demonstrate that the differences are due to the six cross section models**, not statistics.

Continuous	0.9991316	--------	----------
Multi-Group	0.9169121	-0.0822	8.2%
Unshielded	0.9169121	-0.0822	8.2%
Multi-Band	1.0046517	0.0055	0.5%
Totally Shielded	1.0302999	0.0339	3.3%
Partial Shielded	0.9821768	-0.0170	1.7%

The four multi-group models are well in excess 0.1% differences (from 17 up to 82 TIMES). Multi-Band, 2 Band, results differ by 0.5%; extending to 3 Bands eliminates even this difference and achieves our 0.1% goal. I know of no similar improvement I can make to any of the four multi-group models.

Continuous

Average 0.9991316 +/-0.0002700
Lowest 0.9980110 -0.0011206
Highest 0.9999790 0.0008474

Sample Width Range		Occurrences	Per-Cent Occurred	Per-Cent Normal
-4	-3	1	1.000	0.132
-3	-2	1	1.000	2.140
-2	-1	13	13.000	13.591
-1	0	31	31.000	34.134
0	1	37	37.000	34.134
1	2	13	13.000	13.591
2	3	4	4.000	2.140
Sum		100		

Multi-Band (2 Bands)

Average 1.0046517 +/-0.0007666
Lowest 1.0020091 -0.0026446
Highest 1.0067325 0.0020808

Sample Width Range		Occurrences	Per-Cent Occurred	Per-Cent Normal
-3	-2	4	4.000	2.140
-2	-1	15	15.000	13.591 -
1	0	31	31.000	34.134
0	1	37	37.000	34.134
1	2	12	12.000	13.591
2	3	2	2.000	2.140
Sum		100		

Multi-Group

Average 0.9169121 +/-0.0002659
Lowest 0.9161100 -0.0008021
Highest 0.9178380 0.0009259

Sample Width Range		Occurrences	Per-Cent Occurred	Per-Cent Normal
-3	-2	4	4.000	2.140
-2	-1	12	12.000	13.591
-1	0	34	34.000	34.134
0	1	31	31.000	34.134
1	2	18	18.000	13.591
2	3	1	1.000	2.140
Sum		100		

Totally Shielded

Average 1.0302999 +/-0.0002789
Lowest 1.0294000 -0.0008999
Highest 1.0311700 0.0008701

Sample Width Range		Occurrences	Per-Cent Occurred	Per-Cent Normal
-3	-2	3	3.000	2.140
-2	-1	17	17.000	13.591
-1	0	26	26.000	34.134
0	1	42	42.000	34.134
1	2	9	9.000	13.591
2	3	3	3.000	2.140
Sum		100		

Unshielded

Average 0.9169121 +/-0.0002659
Lowest 0.9161100 -0.0008021
Highest 0.9178380 0.0009259

Sample Width Range		Occurrences	Per-Cent Occurred	Per-Cent Normal
-3	-2	4	4.000	2.140
-2	-1	12	12.000	13.591
-1	0	34	34.000	34.134
0	1	31	31.000	34.134
1	2	18	18.000	13.591
2	3	1	1.000	2.140
Sum		100		

Partially Shielded

Average 0.9821768 +/-0.0002671
Lowest 0.9814710 -0.0007058
Highest 0.983372 0.0011952

Sample Width Range		Occurrences	Per-Cent Occurred	Per-Cent Normal
-3	-2	3	3.000	2.140
-2	-1	12	12.000	13.591
-1	0	31	31.000	34.134
0	1	41	41.000	34.134
1	2	10	10.000	13.591
2	3	2	2.000	2.140
3	4	1	1.000	0.132
Sum		100		

311 ^{235}U Slow Critical Assemblies

1	HMT001-1	U235	Poly		66	HST006-14	U235	Nickel	
2	HMT008-D	U235	Poly		67	HST006-15	U235	Nickel	
3	HMT008-S	U235	Poly		68	HST006-16	U235	Nickel	
4	HST001-1	U235	Bare		69	HST006-17	U235	Nickel	
5	HST001-2	U235	Bare		70	HST006-18	U235	Ni-Borated-H2O	
6	HST001-3	U235	Bare		71	HST006-19	U235	Ni-Borated-H2O	
7	HST001-4	U235	Bare		72	HST006-20	U235	Ni-Borated-H2O	
8	HST001-5	U235	Bare		73	HST006-21	U235	Ni-Borated-H2O	
9	HST001-6	U235	Bare		74	HST006-22	U235	Borated-H2O	
10	HST001-7	U235	Bare		75	HST006-23	U235	Borated-H2O	
11	HST001-8	U235	Bare		76	HST006-24	U235	Borated-H2O	
12	HST001-9	U235	Bare		77	HST006-25	U235	Borated-H2O	
13	HST001-10	U235	Bare		78	HST006-26	U235	Borated-H2O	
14	HST002-1	U235	Steel	case	79	HST006-27	U235	Nickel&	H2O
15	HST002-2	U235	Steel	case	80	HST006-28	U235	Nickel&	H2O
16	HST002-3	U235	Steel	case	81	HST006-29	U235	Nickel&	H2O
17	HST002-4	U235	Steel	case	82	HST009-1	U235	H2O	
18	HST002-5	U235	Al	case	83	HST009-2	U235	H2O	
19	HST002-6	U235	Al	case	84	HST009-3	U235	H2O	
20	HST002-7	U235	Al	case	85	HST009-4	U235	H2O	
21	HST002-8	U235	Al	case	86	HST010-1	U235	H2O	
22	HST002-9	U235	Al	case	87	HST010-2	U235	H2O	
23	HST002-10	U235	Al	case	88	HST010-3	U235	H2O	
24	HST002-11	U235	Al	case	89	HST010-4	U235	H2O	
25	HST002-12	U235	Al	case	90	HST011-1	U235	Spherical	
26	HST002-13	U235	Al	case	91	HST011-2	U235	Spherical	
27	HST002-14	U235	Al	case	92	HST012-1	U235	H2O	
28	HST003-1	U235	Poly		93	HST013-1	U235	ORNL-1	
29	Hst003-2	U235	Poly		94	HST013-2	U235	ORNL-2	
30	Hst003-3	U235	Poly		95	HST013-3	U235	ORNL-3	
31	Hst003-4	U235	Poly		96	HST013-4	U235	ORNL-4	
32	Hst003-5	U235	Poly		97	HST014-1	U235	H2O	
33	Hst003-6	U235	Poly		98	HST014-2	U235	H2O	
34	Hst003-7	U235	Poly		99	HST014-3	U235	H2O	
35	Hst003-8	U235	Poly		100	HST015-1	U235	H2O	
36	Hst003-9	U235	Poly		101	HST015-2	U235	H2O	
37	Hst003-10	U235	Poly		102	HST015-3	U235	H2O	
38	Hst003-11	U235	Poly		103	HST015-4	U235	H2O	
39	Hst003-12	U235	Poly		104	HST015-5	U235	H2O	
40	Hst003-13	U235	Poly		105	HST016-1	U235	H2O	
41	Hst003-14	U235	Poly		106	HST016-2	U235	H2O	
42	Hst003-15	U235	Poly		107	HST016-3	U235	H2O	
43	Hst003-16	U235	Poly		108	HST017-1	U235	H2O	
44	Hst003-17	U235	Poly		109	HST017-2	U235	H2O	
45	Hst003-18	U235	Poly		110	HST017-3	U235	H2O	
46	Hst003-19	U235	Poly		111	HST017-4	U235	H2O	
47	HST004-1	U235	27cm-D2O		112	HST017-5	U235	H2O	
48	HST004-2	U235	26cm-D2O		113	HST017-6	U235	H2O	
49	HST004-3	U235	25cm-D2O		114	HST017-7	U235	H2O	
50	HST004-4	U235	24cm-D2O		115	HST017-8	U235	H2O	
51	HST004-5	U235	22cm-D2O		116	HST018-1	U235	H2O	
52	HST004-6	U235	30cm-D2O		117	HST018-2	U235	H2O	
53	HST006-1	U235	Air		118	HST018-3	U235	H2O	
54	HST006-2	U235	Air		119	HST018-4	U235	H2O	
55	HST006-3	U235	Air		120	HST018-5	U235	H2O	
56	HST006-4	U235	Air		121	HST018-6	U235	H2O	
57	HST006-5	U235	Air		122	HST018-7	U235	H2O	
58	HST006-6	U235	Air		123	HST018-8	U235	H2O	
59	HST006-7	U235	Air		124	HST018-9	U235	H2O	
60	HST006-8	U235	Water		125	HST018-10	U235	H2O	
61	HST006-9	U235	Water		126	HST018-11	U235	H2O	
62	HST006-10	U235	Water		127	HST018-12	U235	H2O	
63	HST006-11	U235	Water		128	HST019-1	U235	H2O	
64	HST006-12	U235	Nickel		129	HST019-2	U235	H2O	
65	HST006-13	U235	Nickel		130	HST019-3	U235	H2O	

311 ^{235}U Slow Critical Assemblies (continued)

131	HST020-1	U235	Bare
132	HST020-2	U235	Bare
133	HST020-3	U235	Bare
134	HST020-4	U235	Bare
135	HST020-5	U235	Bare
136	Hst025-1	U235	Water
137	Hst025-2	U235	Water
138	Hst025-3	U235	Water
139	Hst025-4	U235	Water
140	Hst025-5	U235	Water
141	Hst025-6	U235	Water
142	Hst025-7	U235	Water
143	Hst025-8	U235	Water
144	Hst025-9	U235	Water
145	Hst025-10	U235	Water
146	Hst025-11	U235	Water
147	Hst025-12	U235	Water
148	Hst025-13	U235	Water
149	Hst025-14	U235	Water
150	Hst025-15	U235	Water
151	Hst025-16	U235	Water
152	Hst025-17	U235	Water
153	Hst025-18	U235	Water
154	Hst027-1	U235	Bare
155	Hst027-2	U235	B4C-rod
156	Hst027-3	U235	B4C-rod
157	Hst027-4	U235	B4C-rod
158	Hst027-5	U235	B4C-rod
159	Hst027-6	U235	Cd-rod
160	Hst027-7	U235	Cd-rod
161	Hst027-8	U235	Cd-rod
162	Hst027-9	U235	Cd-rod
163	Hst028-1	U235	Water
164	Hst028-2	U235	Water
165	Hst028-3	U235	Water
166	Hst028-4	U235	Water
167	Hst028-5	U235	Water
168	Hst028-6	U235	Water
169	Hst028-7	U235	Water
170	Hst028-8	U235	Water
171	Hst028-9	U235	Water
172	Hst028-10	U235	Water
173	Hst028-11	U235	Water
174	Hst028-12	U235	Water
175	Hst028-13	U235	Water
176	Hst028-14	U235	Water
177	Hst028-15	U235	Water
178	Hst028-16	U235	Water
179	Hst028-17	U235	Water
180	Hst028-18	U235	Water
181	Hst029-1	U235	Water
182	Hst029-2	U235	Water
183	HST029-3	U235	Water
184	Hst029-4	U235	Water
185	Hst029-5	U235	Water
186	Hst029-6	U235	Water
187	Hst029-7	U235	Water
188	Hst030-1	U235	Water
189	Hst030-2	U235	Water
190	Hst030-3	U235	Water
191	Hst030-4	U235	Water
192	Hst030-5	U235	Water
193	Hst030-6	U235	Water
194	Hst030-7	U235	Water
195	HST032-1	U235	ORNL-10
196	HST042-1	U235	solution
197	HST042-2	U235	solution
198	HST042-3	U235	solution
199	HST042-4	U235	solution
200	HST042-5	U235	solution
201	HST042-6	U235	solution
202	HST042-7	U235	solution
203	HST042-8	U235	solution
204	HST043-1	U235	solution
205	HST043-2	U235	solution
206	HST043-3	U235	solution
207	LCT006-1	U235	Water
208	LCT006-2	U235	Water
209	LCT006-3	U235	Water
210	LCT006-4	U235	Water
211	LCT006-5	U235	Water
212	LCT006-6	U235	Water
213	LCT006-7	U235	Water
214	LCT006-8	U235	Water
215	LCT006-9	U235	Water
216	LCT006-10	U235	Water
217	LCT006-11	U235	Water
218	LCT006-12	U235	Water
219	LCT006-13	U235	Water
220	LCT006-14	U235	Water
221	LCT006-15	U235	Water
222	LCT006-16	U235	Water
223	LCT006-17	U235	Water
224	LCT006-18	U235	Water
225	LMT001	U-nat	D2O
226	LMT002-1	U235	D2O
227	LMT002-2	U235	D2O
228	LMT002-3	U235	D2O
229	LMT002-6	U235	D2O
230	LMT002-10	U235	D2O
231	LMT002-11	U235	D2O
232	LMT002-12	U235	D2O
233	LST001	U235	Sheba-11
234	LST002-1	U235	15cm-H2O
235	LST002-2	U235	Bare
236	LST002-3	U235	15cm-H2O
237	LST003-1	U235	Bare
238	LST003-2	U235	Bare
239	LST003-3	U235	Bare
240	LST003-4	U235	Bare
241	LST003-5	U235	Bare
242	LST003-6	U235	Bare
243	LST003-7	U235	Bare
244	LST003-8	U235	Bare
245	LST003-9	U235	Bare
246	LST004-1	U235	30cm-H2O
247	LST004-2	U235	30cm-H2O
248	LST004-3	U235	30cm-H2O
249	LST004-4	U235	30cm-H2O
250	LST004-5	U235	30cm-H2O
251	LST004-6	U235	30cm-H2O
252	LST004-7	U235	30cm-H2O
253	LST005-1	U235	H2O
254	LST005-2	U235	H2O
255	LST005-3	U235	H2O
256	LST007-1	U235	Bare
257	LST007-2	U235	Bare
258	LST007-3	U235	Bare
259	LST007-4	U235	Bare
260	LST007-5	U235	Bare

311 ^{235}U Slow Critical Assemblies (continued)

261	LST009-1	U235	Concrete	287	LST019-3	U235	Poly
262	LST008-1	U235	Concrete	288	LST019-4	U235	Poly
263	LST008-2	U235	Concrete	289	LST019-5	U235	Poly
264	LST008-3	U235	Concrete	290	LST019-6	U235	Poly
265	LST008-4	U235	Concrete	291	LST020-1	U235	H2O
266	LST009-2	U235	Concrete	292	LST020-2	U235	H2O
267	LST009-3	U235	Concrete	293	LST020-3	U235	H2O
268	LST010-1	U235	Poly	294	LST020-4	U235	H2O
269	LST010-2	U235	Poly	295	LST021-1	U235	Bare
270	LST010-3	U235	Poly	296	LST021-2	U235	Bare
271	LST010-4	U235	Poly	297	LST021-3	U235	Bare
272	LST016-1	U235	30cm-H20	298	LST021-4	U235	Bare
273	LST016-2	U235	30cm-H20	299	LST022-1	U235	case-136
274	LST016-3	U235	30cm-H20	300	LST022-2	U235	case-135
275	LST016-4	U235	30cm-H20	301	LST022-3	U235	case-134
276	LST016-5	U235	30cm-H20	302	LST022-4	U235	case-138
277	LST016-6	U235	30cm-H20	303	LST023-1	U235	TwoTanks
278	LST016-7	U235	30cm-H20	304	LST023-2	U235	TwoTanks
279	LST017-1	U235	Bare	305	LST023-3	U235	TwoTanks
280	LST017-2	U235	Bare	306	LST023-4	U235	TwoTanks
281	LST017-3	U235	Bare	307	LST023-5	U235	TwoTanks
282	LST017-4	U235	Bare	308	LST023-6	U235	TwoTanks
283	LST017-5	U235	Bare	309	LST023-7	U235	TwoTanks
284	LST017-6	U235	Bare	310	LST023-8	U235	TwoTanks
285	LST019-1	U235	Poly	311	LST023-9	U235	TwoTanks
286	LST019-2	U235	Poly				

Boundary Conditions

Physically the correct boundary conditions are simple to state: we require continuity of the neutron flux, using continuous energy, multi-group or multi-band cross sections.

This is EXTREMLY important, because the results in this paper, and other related papers, indicate that the reason the Probability Table Method (PTM) and Multi-Band Method (MB), with all of their apparent approximations, are so successful is not because of what is happening inside the fuel, but rather by improving what's incident and reflected on the surface of the fuel; all this needs is the correct distribution of total cross sections, and is independent of the NR, SLBW, and other limitations of PTM and MB. As shown in the above figures, this is something **Continuous** energy cross sections, and **Multi-Band** cross section can do, for thin and thick systems, but **Multi-Group**, with only one degree of freedom per group, cannot do.

With **Monte Carlo** codes this is easy for us to accomplish: in TART after each "event" (be it a source, collision, fission, etc.) I sample cross sections for **each isotope** that the neutron encounters. I then use these cross sections until the next "event", regardless of how many different spatial zones the neutron may pass through between "events". For example, in the above simple Uranium/water assembly, if an "event" occurs in the Uranium I separately sample ^{235}U and ^{238}U cross sections, which is all I need to start tracking the neutron. If the neutron leaves the Uranium and enters the water, I sample H and O cross sections and continue tracking. If the neutron track leaves the water and enters another Uranium zones, I know that I have already sampled the ^{235}U and ^{238}U, so I need not sample any more cross sections to continue tracking the neutron. **This cross section "memory" is imperative to accomplish the correct boundary conditions** (Nikolaev's all the way method [23]); easy to do in a Monte Carlo code. Consider the multi-band method using only 2 bands, I'll refer to these as the smaller and larger totals. If in the first Uranium zone I randomly select the smaller cross section this greatly increases the probability that the neutron will leak from the Uranium, transport through the water, and enter a second Uranium pin. It is then **imperative** that in the second Uranium pin we continue to use the already sampled smaller cross section. This is the only way we can guarantee satisfying the correct boundary conditions and correctly define the so called Dancoff correction factor for the coupling between surrounding fuel pins. If we mistakenly re-sample the Uranium cross section when entering the second pin, we lose the strong correlation to leakage from the first pin, and overestimate the ^{235}U and ^{238}U cross sections, immediately overestimating the reaction rate from the surface and into the second pin.

With **multi-group** codes continuity of the **multi-group** flux at boundary is easy to accomplish. Unfortunately, continuity of **multi-band** flux is much more difficult. The analogy to the method I described above for Monte Carlo infers 2 bands for each isotope, and per group: with N isotopes we end up with 2^N cross section bands. For the simple U/water example with 4 evaluations, 2^4, or 16 bands per group; for a problem with 10 isotopes (more realistic), 2^{10}, or 1,204 bands per group (Nikolaev's all the way method [23]). While theoretically correct, for any real problems this quickly becomes impractical in a deterministic code; this is an obvious advantage of Monte Carlo over multi-group. However, multi-group is still so widely used it is worth investigating approximate boundary conditions.

The above results demonstrate accuracy problems with standard multi-group methods, but these results can be improved by focusing on the source of the differences, which is self-shielding in the fuel. For example, much of the difference can be eliminated by using 2 bands in the fuel, to correct self-shielding, and normal multi-group cross sections in the water. For the simple U/water presented here I prepared 2 band cross sections for the Uranium mixture (2% ^{235}U, 98% ^{238}U). This accounts for self-shielding and calculates K_{eff} values very similar to those I calculate with the standard multi-band TART method, described above.

Infinite and Homogeneous

The simple example presented earlier is an **infinite** system, but it is not **infinite** and **homogeneous**, which, by ignoring the spatial and directional effect, μK, is what the multi-group models presented here assume. But obviously the simple example is a heterogeneous system, with separate layers of Uranium and Water; here we expect large spatially currents between the Uranium and Water, as shown in the above plots of flux and reactions. In this case ignoring the spatial and directional effect, μK, would seem to be difficult to justify.

In order to show how heterogeneous effects self-shielding, I homogenized the simple example of Uranium and Water, by mixing the two together, and changing the ^{235}U enrichment to make the resulting homogeneous system close to critical.

Cross Section Presentation	Infinite K-eff	Difference	Infinite & Homogeneous K-eff	Difference
Continuous	0.999924	--------	0.999816	--------
Multi-Group	0.974683	-0.025241	0.966235	-0.033581
Multi-Band	1.000980	0.001056	1.000680	0.000864
Unshielded	0.974645	-0.025279	0.966169	-0.033647
Total Shielded	1.001750	0.001826	0.999059	-0.000757
Partial Shielded	0.991570	-0.008354	0.986059	-0.013757

The above table shows the heterogenous (identical to the earlier table) and homogeneous results side-by-side. The results to note include,

1) Unshielded results show BIG differences: heterogenous 2.52% ; homogeneous3.35% .
2) Partial Shielding yields mixed results: heterogeneous 0.8%; homogenous 1.3%.
3) Totally Shielding in heterogeneous within 0.2%; homogeneous is within 0.1%.
4) In both cases, Multi-Band is near or within 0.1%.

The bottom line is that,

1) Self-shielding is always important; failure to include it results in **differences in K_{eff} over 25 to 22 TIMES the 0.1 we believe we can achieve**.
2) Standard multi-group self-shielding improves K_{eff} results close to 0.1; here 0.1 to 0.2.
3) Only Multi-band agrees within or close to 0.1.

Beyond these K_{eff} results, I will remind readers of the important spatial and directional effects seen in the above plots; standard multi-group results differ by large factors, whereas multi-band results agree much closer for both thin and thick systems. **This would suggest that if you are interested in spatially dependent effects, such as fuel burnup, normal multi-group is not for you. Whereas continuous and/or multi-band will need your needs.**

Homogeneous: Analog Events vs. Isotope per Removed Neutron

Continuous

Reaction	92235	92238	1001	8016
Elastic	1.36013	26.23770	0.61951	0.12478
(n,n')	0.16432	3.49912	0.00000	0.00001
(n,2n)	0.00021	0.00432	0.00000	0.00000
(n,3n)	0.00000	0.00002	0.00000	0.00000
(n,4n)	0.00000	0.00000	0.00000	0.00000
Fission	0.27713	0.10661	0.00000	0.00000
(n,n'a)	0.00000	0.00000	0.00000	0.00000
(n,p)	0.00000	0.00000	0.00000	0.00000
(n,a)	0.00000	0.00000	0.00000	0.00004
(n,g)	0.06680	0.54486	0.00001	0.00000
Totals	1.86859	30.39260	0.61952	0.12483

Homogeneous: Analog Removal and Production per Removed Neutron

The above table of results are **Expected,** and the below table are **Analog**; note the agreement in all cases to well within 3 digits (yet another indicator of convergence).

Expected 0.999924
Analog 0.999874

Continuous

Reaction	Removal	Production	Events
Elastic	0.000000	0.000000	28.342100
(n,n')	0.000000	0.000000	3.663460
(n,2n)	0.004535	0.009070	0.004535
(n,3n)	0.000024	0.000072	0.000024
(n,4n)	0.000000	0.000000	0.000000
Fission	0.383742	0.990734	0.383742
(n,n'a)	0.000000	0.000000	0.000000
(n,p)	0.000000	0.000000	0.000000
(n,a)	0.000036	0.000000	0.000036
(n,g)	0.611665	0.000000	0.611665
Leakage	0.000000	0.000000	0.000000
Totals	1.000000	0.999876	33.005600
K-eff		0.999874	

The Unresolved Resonance Region

Even codes that use continuous energy cross sections, must account for self-shielding in the ENDF-102 unresolved resonance region (URR) [1]. In earlier papers [5, 6] we address this point, using NJOY [16] and MCNP [4], with and without self-shielding in the URR. The following test were performed.

First, we demonstrated the importance of self-shielding in the URR by performing MCNP [4] calculations of 32 critical assemblies with and without URR self-shielding; all these results are based on running an unmodified version of MCNP. The following results are for,

1) Not including URR self-shielding (SS), i.e., using unshielded, or infinitely dilute.
2) Using the Probability Table Method (PTM), with 20 cross section bands [24, 25].
3) Using the Multi-Band Method, using only 2 cross section bands.

On the below figure the MCNP PTM +/- 0.1% lines are included merely as eye guides.

In the below figure the crit # corresponds to the numbers in the critical assembly in following table. Even without identifying the individual assemblies the below figure clearly shows that,

1) In these cases, unresolved region self-shielding (URR SS) had an important macroscopic effect on the results. **Here we see that if we do not account for URR SS the answers can be up to 1% different** from the standard MCNP results with URR SS, well outside the accuracy we are attempting to achieve.

2) In ALL these cases **the results using 20 PTM bands or 2 MB bands are indistinguishable**, well within 0.1% of one another; indeed, almost ALL are within 0.02% of one another, far below the level of agreement we require in our applications.

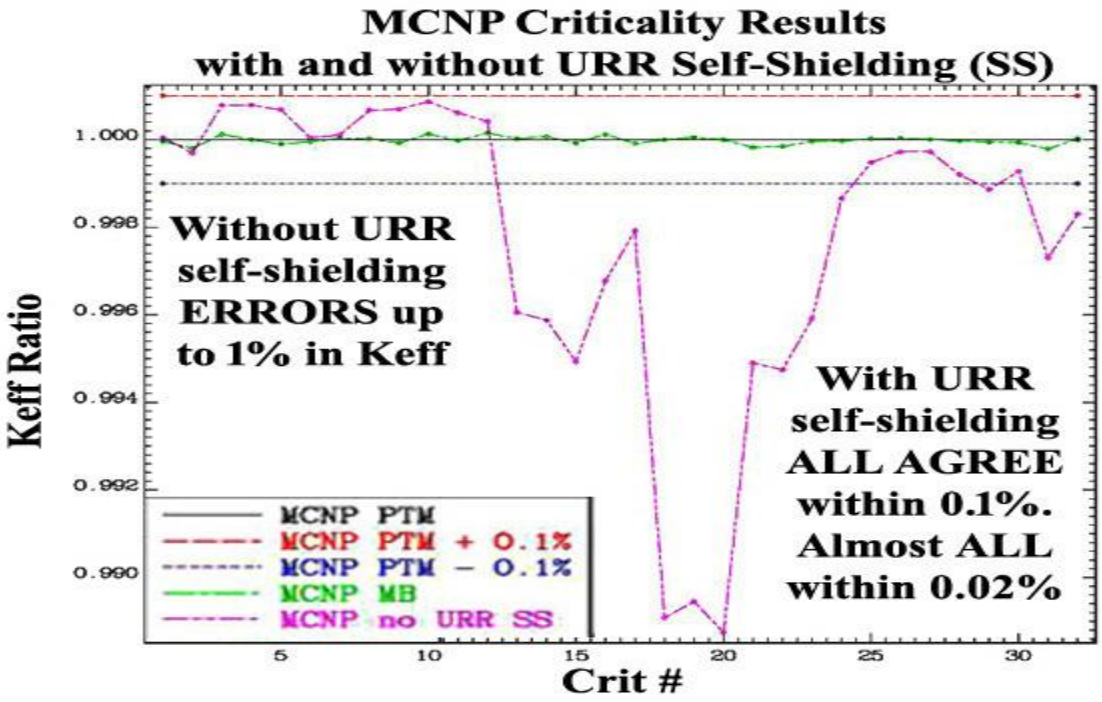

32 Critical Assemblies used for MCNP Results

Crit #	ICSBEP label	Short name	Common name
1	HEU-MET-FAST-001	hmf001	Godiva
2	HEU-MET-FAST-002	hmf002-2	Topsy-2
3	HEU-MET-FAST-003	hmf003-01	Topsy-U_2.0in(Uranium reflector)
4	HEU-MET-FAST-003	hmf003-02	Topsy-U_3.0in(Uranium reflector)
5	HEU-MET-FAST-003	hmf003-03	Topsy-U_4.0in(Uranium reflector)
6	HEU-MET-FAST-003	hmf003-10	Topsy-W_4.5in(Tungsten reflector)
7	HEU-MET-FAST-003	hmf003-11	Topsy-W_6.5in(Tungsten reflector)
8	HEU-MET-FAST-014	hmf014	VNIIEF-CTF-DU
9	HEU-MET-FAST-032	hmf032-1	COMET-TU1_3.93in
10	HEU-MET-FAST-032	hmf032-2	COMET-TU1_3.52in
11	HEU-MET-FAST-032	hmf032-3	COMET-TU1_1.742in
12	HEU-MET-FAST-032	hmf032-4	COMET-TU1-0.683in
13	IEU-MET-FAST-007	imf007	Big_Ten
14	IEU-MET-FAST-007	imf007d	Big_Ten(detailed)
15	IEU-MET-FAST-010	imf010	ZPR-6/9(U9)
16	IEU-MET-FAST-013	imf013	ZPR-9/1(Tungsten reflector)
17	IEU-MET-FAST-014	imf014-2	ZPR-9/2(Tungsten reflector)
18	MIX-MISC-FAST-001	mif001-01	BFS-35-1
19	MIX-MISC-FAST-001	mif001-02	BFS-35-2
20	MIX-MISC-FAST-001	mif001-03	BFS-35-3
21	MIX-MISC-FAST-001	mif001-09	BFS-31-4
22	MIX-MISC-FAST-001	mif001-10	BFS-31-5
23	MIX-MISC-FAST-001	mif001-11	BFS-42
24	IEU-MET-FAST-022	imf022-01	FR0_3X-S
25	IEU-MET-FAST-022	imf022-02	FR0_5-S
26	IEU-MET-FAST-022	imf022-03	FR0_6A-S
27	IEU-MET-FAST-022	imf022-04	FR0_7-S
28	IEU-MET-FAST-022	imf022-05	FR0_8-S
29	IEU-MET-FAST-022	imf022-06	FR0_9-S
30	IEU-MET-FAST-022	imf022-07	FR0_10-S
31	IEU-MET-FAST-012	imf012	ZPR-3/41
32	IEU-COMP-FAST-004	icf004	ZPR-3/12

The reason the 2 band Multi-Band results produces results equivalent to 20 band PTM results is in the difference between how the bands and weights are defined: Multi-Band explicitly conserves expected limiting values of the total cross section (exactly, without any statistics), while PTM does not explicitly conserve anything (it randomly samples ladders to within some statistical level). For more on this topic, see details in refs. [5, 6], and/or the brief summary in the Appendix on PTM vs. MB Methods.

Conclusions

In this paper I describe why Resonance Self-Shielding is so important, and I present examples to illustrate the magnitude of this effect. More importantly, in order to improve the accuracy of our results, I address what can be done to improve our treatment of self-shielding. Throughout I use recent ENDF data [1, 2], and Monte Carlo codes TART [3], and MCNP [4].

I point out the difference between Monte Carlo and deterministic codes (e.g., Sn), as it relates to how each treat self-shielding; particularly regarding boundary conditions. By definition self-shielding means using energy averaged cross sections: obviously this applies to multi-group codes, but it also applies even to codes that use continuous energy cross sections [3, 4], to correctly include self-shielding in the unresolved resonance region [5. 6].

Lastly, I address the question of the statistical accuracy of Monte Carlo codes, and I present numerous examples, both very simple theoretical results, and hundreds of critical assemblies.

Please note that today our computers are fast enough and large enough that for my own applications with my TART Monte Carlo code [3], I always use Continuous energy cross sections, not multi-group. Therefore, self-shielding is no longer a problem I must deal with, except in the unresolved resonance region [5, 6], where an "energy average" statistical approach is still required and used by both TART [3], and MCNP [4], see the appendix for details.

My conclusions include,

1) Failure to account for resonance self-shielding can give RUBBISH results. When you use unshielded cross sections be aware: **The results from any computer code can be no better than the data they use**; with unshielded cross sections you can in a: "garbage in = garbage out", situation.
2) Standard methods of self-shielding in principle only apply to infinite, homogeneous media, but in practice they produce surprisingly accurate results for integral parameters, such as K_{eff}. However, they fail to accurately account for important spatial and directional results simultaneously for thick and thin media, such as spatially dependent fuel burn-up.
3) The multi-band method is designed to accurately reproduce both integral parameters, such as K_{eff}, as well as spatial and directional results, for media which are optically thick or thin media (multi-group does not) and generally agrees with results based on using continuous energy cross sections.

The multi-band method used by TART [3] is used at all neutron energies, whereas with MCNP [4] the Probability Table Method (PTM), is only used define to self-shielding in the unresolved energy range. The multi-band method owes much to the earlier work of Nikolaev [23] and Levitt [24, 25]; it differs in providing an analytical solution to the multi-band equations, to explicitly conserve expected moments of the flux and reaction rates, and in using Monte Carlo [3], to make practical the correct, all important, boundary conditions, ala Nikolaev's all the way approach [23]. The results included in this report are based on using the multi-band method in the TART Monte Carlo code [3] for over 40 years, during which time it has been applied to thousands of applications.

Acknowledgment

I thank **Dave Heinrichs** and **Jesse Norris** (LLNL) for reviewing and publishing this report through LLNL. I also thank **Andrej Trkov** for reviewing my earlier 2019 report on self-Shielding and making many helpful suggestions, which were incorporated into the published report. In also thank **Andrej Trkov** and **Kira Nathani**, for editing and producing the final version of my 2019 paper as an IAEA report.

References

[1] "**ENDF-6 Formats Manual** Data Formats and Procedures for the Evaluated Nuclear Data File ENDF/B-VI and ENDF/B-VII", Written by the Members of the Cross Sections Evaluation Working Group; Last Revision, Edited by M. Herman and A. Trkov, February 2018.

[2] **"ENDF/B-VII.0:** Next Generation Evaluated Nuclear Data Library for Nuclear Science and Technology", with M.B. Chadwick and many others, Nucl. Data Sheets **107** (2006), and "**ENDF/B-VIII.0**: The 8th Major Release of the Nuclear Reaction Data Library with CIELO-project Cross Sections, New Standards and Thermal Scattering Data", with D.A.Brown and many others, Nucl. Data Sheets **148** (2018).

[3] "**TART 2016**: An Overview of a Coupled Neutron-Photon 3-D, Combinatorial Geometry Time Dependent Monte Carlo Transport Code", Report: LLNL-SM-704560, Code Release: LLNL-CODE-708759, September 2016.

[4] "**MCNP** - A General Monte Carlo N-Particle Transport Code", Version 5, Vol. I: Overview and Theory, X-5 Monte Carlo Team, Los Alamos National Laboratory report LA-UR-03-1987 (April 24, 2003).

[5] "**An Alternate Approach to Creating ACE** Files for Use in Monte Carlo Codes", INDC(NDS)-0701, December 2015, Nuclear Data Section, IAEA, Vienna, Austria. https://www-nds.iaea.org/publications/indc/indc-nds-0701/

[6] "**URR-PACK**: Calculating Self-Shielding in the Unresolved Resonance Energy Range", INDC(NDS)-0711, Rev. 1, July 2016, Nuclear Data Section, IAEA, Vienna, Austria. https://www-nds.iaea.org/publications/indc/indc-nds-0711/

[7] "**PREPRO2017**: 2017 ENDF/B Pre-processing Codes", IAEA-NDS-39, Rev. 17, May 2017. (ENDF/B-VII or Proposed VIII Tested); codes are freely available on-line at, http://redcullen1.net/HOMEEPAGE.NEW/index.htm

[8] "**POINT2018**: ENDF/B-VIII Final Temperature Dependent Cross Section Library", IAEA-NDS-227, April 2018, Nuclear Data Section (NDS), IAEA, Vienna, Austria. https://www-nds.iaea.org/publications/nds/iaea-nds-0227/

[9] "ENDF/B-VII.0 Data Testing Using **1,172 Critical Assemblies**", Lawrence Livermore National Laboratory, UCRL-TR-235178, October 2007

[10] "Application of the **Probability Table Method** in multi-group calculations", BNL-50387 (ENDF-187), May 1973.

[11] "Application of the **Probability Table Method** to Multi-Group Calculations," Nuc. Sci. Eng. **56**, 387-400 (1974).

[12] "Direct Calculation of **Cross Section Probability Tables**", Trans. Amer. Nucl. Soc. **23**, 526 (1976).

[13] "Calculation of Probability Table Parameters to Include **Intermediate Resonance** Self-Shielding," Lawrence Livermore Laboratory Report UCRL-79761, San Francisco, CA, December 1977.

[14] D.E. Cullen, Yigal Ronen (Ed.): "**Nuclear Cross Section Processing**", Handbook of Nuclear Reactor Calculation, vol. I, CRC Press, Inc., Boca Raton, Florida (1986).

[15] D.E.Cullen, "**Nuclear Data Preparation**", pp. 279-425, Vol. 1, in: "The Handbook of Nuclear Engineering", Springer Publishing, NY, NY (2010).

[16] R.E. MacFarlane, et al.: The **NJOY** Nuclear Data Processing System, Version 2012, LA-UR-12-27079, August 2013.

[17] **Pu239:** R.L.Bramblett and J.B.Czirr, "Measurements of Fissions Produced in Bulk Plutonium-239 by 2 eV to 10 keV Neutrons", Nucl. Sci. Eng. **28**, 62-71 (1967).

[18] **U235:** R.L.Bramblett and J.B.Czirr, "Energy-Dependent Self-Shielding Factors for U235 Foils from Transmission Measurements", Nucl. Sci. Eng. **35**, 350-357 (1969).

[19] E.F.Plechaty and D.E.Cullen, "Calculation of Resonance Self-Shielding in **U235**", UCID-16359, (1973), Lawrence Livermore National Laboratory.

[20] E.F.Plechaty and D.E.Cullen, "Calculation of Resonance Self-Shielding in **Pu239**", UCID-16433, (1974), Lawrence Livermore National Laboratory.

[21] E.F.Plechaty and D.E.Cullen, "Resonance Self-Shielding Calculations Using the **Probability Table Method**", UCID-17230, (1976), Lawrence Livermore National Laboratory.

[22] with Ernest F. Plechaty, "ENDF/B-VII.0 Data Testing Using **1,172 Critical Assemblies**", Lawrence Livermore National Laboratory, UCRL-TR-235178, October 2007.

[23] Nikolaev, M.N., and Phillipov, V.V., Atomic Energy **15**, 493 (1963).

[24] L.B. Levitt: "The probability table method for treating unresolved resonances in Monte Carlo calculations", BNL-50387 (ENDF-187), May 1972.

[25] L.B. Levitt: "The probability table method for treating unresolved resonances in Monte Carlo calculations", Nucl. Sci. Eng. **49**, No 4, 450-457 (1972).

[26] Stewart, J.C., J. Quant. Spectrosc. Radiat. Transfer **4**, 723 (1964).

[27] Goldstein, R., and Cohen, "Theory of Resonance Absorption of Neutrons", Nucl. Sci. Eng. **13**, 132-140 (1962).

[28] Goldstein, R., "Temperature-Dependent Intermediate Neutron Resonance Integrals", Nucl. Sci. Eng. **48**, 248-254 (1972).

[29] Goldstein, R., Trans. Am. Nucl. Soc. **21**, 493 (1975).

APPENDICES

A Long History of Time

We have come so far since the beginning of ENDF, over 50 years ago, but I fear that today we are repeating some of the mistakes we made and corrected many years ago. When ENDF started the U.S. nuclear data effort was relatively small and uncoordinated, with each Lab or company independently handling their own nuclear data needs. In this situation at each site all the nuclear needs were met by a relatively small number of people, which had the advantage that it was the same people who selected the basic data, processed it, and then used it in their applications. But the lack of coordination meant that it was difficult to compare results or properly test data, in any attempt to improve the basic data. It was so bad that the two main U.S. nuclear reactor producers could each independently design their type of reactor, but they couldn't design the reactor built by the other company, e.g., their codes and nuclear data were incompatible.

One important step in the ENDF effort was to standardize definitions, and document them in the ENDF Formats and Convention Manual, ENDF-102 [1]. This allowed ENDF users to become more specialized, with experts in different areas concentrating strictly on their own area of expertise and relying on everyone else to follow the strict rules and definitions documents in ENDF-102. As a result, today we have on one side experts on nuclear physics producing ENDF data using their nuclear model codes, and on the other side experts on neutron transport codes using their expertise to use this data in their applications.

There are a number of important steps needed to go from evaluated data in the ENDF format to the form it is used in our transport codes. The two extreme ends of the ENDF chain are manned by experts in nuclear physics and measurements, and in creating evaluated data and on the other end of the ENDF chain we have experts on neutron transport codes. But what I see as the weak link "**nuclear data processing**" is a less attractive activity, often performed by individuals with little or no background in either creating evaluations or using the data in transport codes. The result can be limitations in the accuracy of our best neutron transport codes because of the processed data they are supplied directly from the nuclear data processing codes.

Here, in this paper, I focused on but one important point: **resonance self-shielding**, and how it can affect the accuracy of our multi-group neutron transport codes. In the hope that it helps, I will merely repeat what I have been saying for decades,

The results of computer codes can be no more accurate than the input data they use.

Or more bluntly: **Garbage in = garbage out.**

A Brief History of Time

In 1972 I first heard Leo Levitt describe his Probability Table Method (PTM), that handles the effect of self-shielding in the **unresolved resonance region** using Monte Carlo calculations [24, 25]. I immediately saw the potential to use Leo's PTM method **over the entire neutron energy range**, using deterministic codes as well as Monte Carlo codes [3, 4]. Only after my first publication did we (Leo Levitt and I) learn of the earlier work in multi-group transport or diffusion, by Nikolaev and Phillipov for neutrons [23], and Stewart for photons [26]; they originated the idea of within each group characterizing the neutrons or photons by the value of the total cross section with which they interact. We must particularly note the work of Nikolaev, who extensively published on this subject, but unfortunately too many of his publications are not available in the West, in English. I am certainly indebted to the work and ideas of Nikolaev, who kindly made me aware of his works.

When I first saw the Levitt's PTM equations [24, 25], I was working on non-linear problems, so I recognized how to analytically solve these equations to define the multi-band weights and cross sections. By 1975 I had implemented what I call the multi-band (MB) method in our TART Monte Carlo code [3] to account for self-shielding across the entire neutron energy range; including the intermediate resonance (IR) method [27, 28, 29], rather than the narrow resonance (NR) used in PTM. This was only possible by using Monte Carlo, to make handling boundary conditions [23] practical, in combination with my analytical parameters.

By now we have over 40 years of experience using the multi-band method in thousands of different neutron calculations. Over those years I have continued to use TART to compare Monte Carlo results using a variety of models, including continuous energy cross sections, versus multi-band to account for self-shielding, versus multi-group with and without for self-shielding. The work that I was doing I documented in textbooks, such as the Handbook of Nuclear reactor Calculations (1986) [14] and more recently the Handbook of Nuclear Engineering (2010) [15]. Also, over the years I have provided computer codes that could be used by others to prepare nuclear data [7] and perform Monte Carlo calculations [3].

When we started work on this self-shielding problem over 40 years ago, computers were too slow and too small to allow us to routinely use continuous energy cross sections, so at the time we heavily relied on the multi-band method. Today's computers are so much faster and bigger that for all my real applications I use continuous energy cross sections, except in the unresolved resonance region, where statistical sampling is still necessary [23, 24, 25]. Even though I personally no longer use the multi-band method across the entire energy range, here I have tried to briefly summarize these 40 years of experience, in the hope that it saves the reader from having to re-invent the wheel and to allow you to more quickly understand the multi-band method: how and why is works and how to use it, particularly in the hope that this method can be used in deterministic codes.

Probability Table versus Multi-Band Methods

Much of this section have been copied from earlier reports [5, 6]. To better understand the similarities and difference between these two methods, let's look at some real cases, such as ENDF/B-VII.1 ^{235}U and ^{238}U, in the **unresolved resonance region** to see what we are trying to approximate,

Material	Unresolved Energy Range	Most self-shielding = lowest f(0) factor
^{235}U	2.25 to 25 keV	0.9544 ~ 4.6% lower than unshielded
^{238}U	20 to 149 keV	0.8667 ~ 12.3% lower than unshielded

Here we see that the variation of the self-shielded cross section in the unresolved resonance energy. range is quite small, e.g., ^{235}U only a maximum of 4.6% change and ^{238}U only a maximum of 12.3%. These differences are certainly large enough to affect macroscopic quantities, such as K_{eff} for critical assemblies, so that self-shielded in the unresolved resonance energy range is important to include in our calculations. But they are relatively easy to accurately represent with a very low order rational, or Pade approximation [14, 15]**. Indeed, our comparison of K_{eff} for a variety of critical assemblies listed above show that these integrals results are statistically indistinguishable whether we use 20 PTM bands or only 2 MB bands.**

How can only 2 multi-band (MB) bands replace 20 probability table method (PTM) bands and still produce accurate results? It is shown that both methods "look" exactly the same (they are both discrete quadratures), and as such **either can be used in ACE [5] files as input to MCNP [4] without making any changes in MCNP; MCNP doesn't know whether it is using PTM or MB data**, e.g., that's why we were able to obtain ALL of the MCNP results presented here without making ANY – repeat ANY – changes to MCNP . Based on the approximations used by the PTM and MB method both are shown to be using a rational, or Pade, approximation, to represent the self-shielded cross section for all values of $\sum_0$ between zero and infinity. This sounds like a difficult task, but the variation in the self-shielded cross section in the unresolved energy range is quite small, so that even only 2 MB bands are adequate to reproduce integral results that are indistinguishable from the results obtained using 20 PTM bands.

If we look at the self-shielding curve for $\sum_0$ between zero and infinity, using 20 or 2 bins, for **^{235}U** we see differences up to 0.017% at the lower energy limit (2.25 keV) and up to 0.001% at the upper energy limit (25 keV); **the results are essentially indistinguishable**.

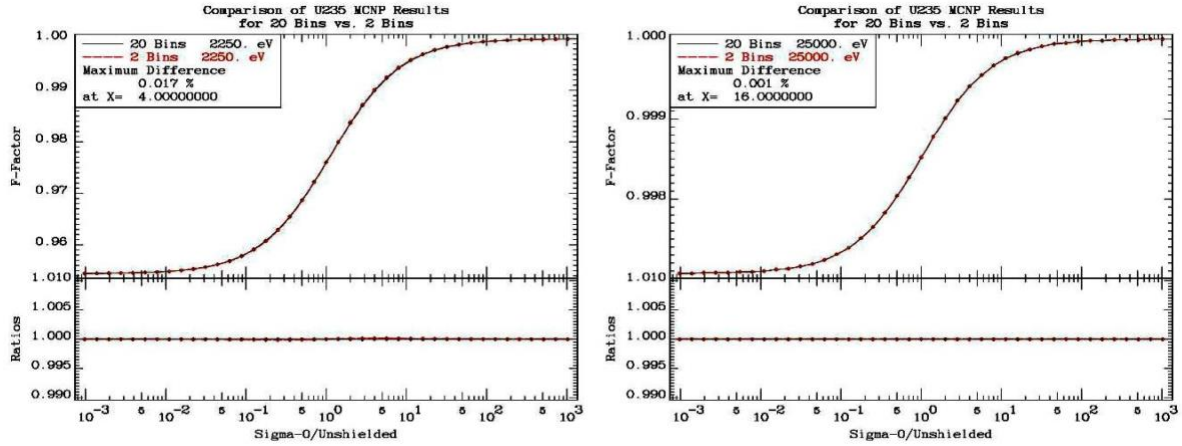

Using 20 or 2 bins, for **^{238}U** we see differences up to 0.328% at the lower energy limit (20 keV) and up to 0.005% at the upper energy limit (near 149 keV); there is a small difference at 20 keV and virtually none at 149 keV. There is little significant difference that affects integral results (which help to explain why we saw no significant difference above for the K_{eff} values).

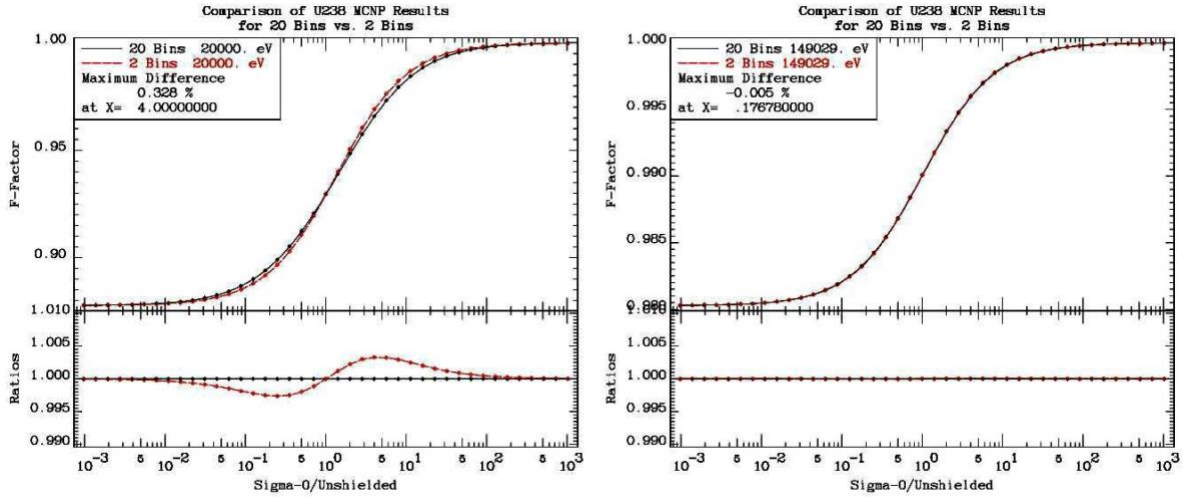

That is not to say that there is anything wrong with the 20 bands and it gives good answers, but for this application 20 bands simply isn't needed; **2 bands are sufficient as long as these 2 band parameters are defined using the multiband definitions to exactly conserve important moments of the flux, as I have done above; AS WITH ANY DISCRETE QUADRATURE, SUCH AS LEGENDRE QUADRATURE USED BY Sn CODES, THAT IS THE KEY.**

If both give the same results, does this means PTM and MB are equivalent? **Please do not make the mistake of assuming they are equivalent, because they ARE NOT.** Also, please do not make the mistake of assuming that PTM and MB results will always agree so closely that their

integral results are essentially indistinguishable, as we found in the above example here. In the above example they both produce statistically identical answers, only because they both used the same approximations.

What the above results show is that in this case the 2 band MB results using only moments from the PTM data, reproduce the 20 band PTM results. In other words, **we do not need 20 bands** to reproduce the rather small changes in the self-shielded cross sections that we see in these cases, i.e., only 4.6% for ^{235}U and 12.3% for ^{238}U.

This does not mean the two methods are equivalent, because PTM uses a number of approximations that MB does not. **In general MB can do much better than this because if we consider all the approximations used by PTM,**

1) MB only needs moments of the cross sections, so there is no statistical uncertainty due to random sampling of a ladder of sampled resonances in PTM [5, 6].
2) By only using moments MB is not restricted to the ENDF restriction to SLBW [1].
3) MB uses the intermediate resonance [27, 28, 29], approximation, not the NR used by PTM [13].
4) MB uses an analytical solution to define the band weights and cross sections [12].
5) MB only uses a few cross sections bands, making practical an extension to deterministic codes, while still satisfying the all-important boundary conditions [14, 15].
6) PTM has only been applied to the unresolved region, whereas MB has been applied across the entire incident neutron energy range [10, 11]; in TART, from 1.0d-5 eV to 20 MeV.

Bondarenko Model

One additional approximation that both PTM and MB use is the Bondarenko approximation, that assumes the resonance structure in each isotope is independent of the resonance structure in all other isotopes; this predicts self-shielding of any mixture of isotopes as $1/[\Sigma_t(E) + <\Sigma_0>]$; $<\Sigma_0>$ represents all other materials. In principle this is an APPROXIMATION strictly valid only for **infinite, homogeneous** media, i.e., $\mu K = 0$. In practice many years of use have proven how accurate it can be to calculate integral parameters, such as Keff.

As applied here it means that when dealing with a mixture of isotopes, both PTM and MB sample the cross sections for each isotope, assuming the resonance structure in each isotope is independent of the resonance structure in all other isotopes. By the definition of "unresolved" that is about the best we can do in the URR. Although I doubt if it is of much importance in the unresolved region, I will merely mention that both PTM and MB cannot account for this effect and as such both are using the Bondarenko approximation. However, when used outside the unresolved energy range we can account for this correlation, in multi-group calculations, e.g., for N cross section bands, an N x N matrix of bands can include conditional probabilities, accounting for "coincidental" correlation. Here we see a BIG, important difference between using PTM with 20 cross section bands, and MB with only 2 bands. A MB 2 x 2 correlation matrix is easy to construct and understand, whereas a PTM 20 x 20 matrix really isn't practical to even consider trying to construct or use.

The below figure compares the TOTAL cross section of Natural Iron (Fe) to the TOTAL cross section of Fe's most abundant isotope, Fe56 (over 91% by atom fraction). Near the 25 keV window in Fe we can see that even though based on atomic fraction Fe56 is dominant, in terms of TOTAL cross section it is only about 1% of the Natural Fe TOTAL cross section. Hopefully this one figure will help you to appreciate, the magnitude of the APPROXIMATION of assuming that when defining self-shielded cross sections for Natural Fe, as an independent sum over its isotopes, for Fe56, we are assuming that the Natural Fe TOTAL can be APPROXIMATED by the Fe56 isotope TOTAL plus some constant $<\Sigma_0>$.

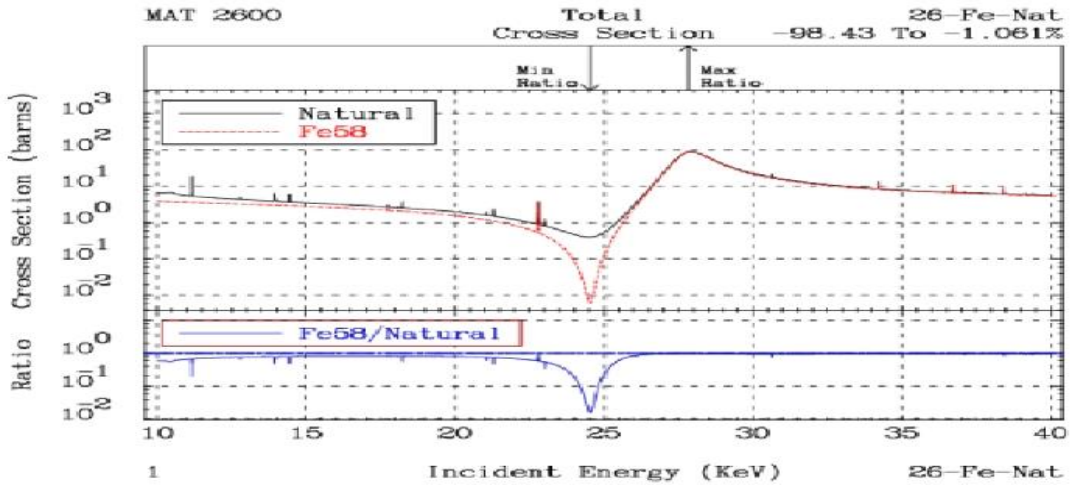

The below figure shows a comparison of the TOTAL cross sections for the Uranium mixture used in the above Simple 1-D model; the Uranium was 2% ^{235}U and 98% ^{238}U. The below figure shows an expanded view of the 4 eV to 100 eV energy range. We see a number of strong, widely spaced ^{238}U resonances (again, 98% of the mix), and more numerous ^{235}U resonances (only 2% of the mix). Here we can see examples of "coincidental" correlation, where rather than sitting on an energy independent $<\Sigma_0>$, the ^{235}U resonances are within the energy range of the strong ^{238}U resonances. From the ratio included in the below figure we can see a number of cases where a $1/\Sigma_t(E)$ weighting drastically changes the contribution of some ^{235}U resonances.

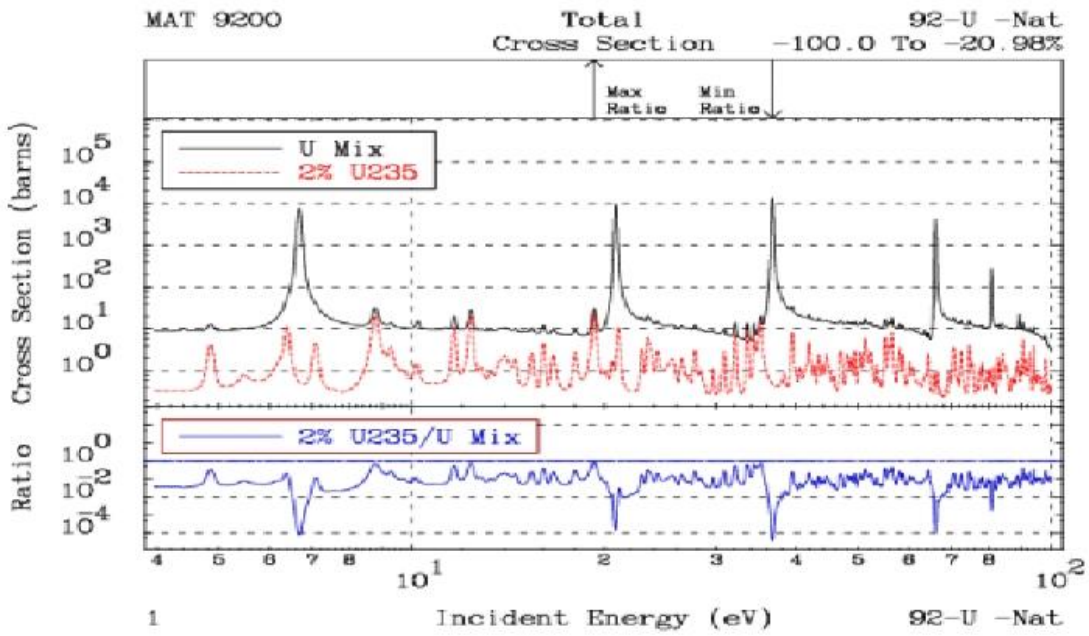

While the Bondarenko approximation has been successfully used for many years to produce processed nuclear data "application independent libraries", today our modern evaluations have so much detail, including thousands and thousands of resonances, there are bound to be groups (ranges of energy) where there is what I refer to as "coincidental" correlation, where resonance just happen to rise or fall in similar patterns. Today our computers are so fast and large and efficient that we really no longer need to use the Bondarenko approximation, e.g., if you want to calculate the self-shielded cross section for any mixture of materials, we now have the computer resources to first define the total cross section of the mixture (e.g., use PREPRO/MIXER [7]) and then use this total as the self-shielding factor to calculate self-shielded cross sections for the individual constituents (use GROUPIE [7]); we need not construct tables of results for a variety of $<\Sigma_0>$; **we can bypass the Bondarenko approach and directly calculate one, unique answer.**

One method successfully used by TART for many years uses MB parameters over the entire energy range, usually 10^{-5} eV up to 20 MeV; not just the unresolved region. Many years of testing and comparison to TART continuous energy cross section treatment, shows that generally only 2 MB bands are needed to account for self-shielding. I mention this here because one the biggest problem with deterministic codes today is accounting for spatial and directional dependent self-shielding.

Over decades deterministic codes have used more and more groups to account for self-shielding; generally, this approach does not work, e.g., ^{238}U would require many thousands of groups and the group-to-group transfer matrix becomes of questionable use/accuracy. **What does work is fewer groups, but 2 cross section bands ala MB in each group.** This is a very practical approach as it can be even more efficient because you will find that you do not need nearly as many groups as you think you do.

Both PTM and MB use a rationale, Pade, approximation [14, 15], as the ratio of two polynomials to define the self-shielded cross section as a smooth continuous function over the entire range of $\Sigma_0 = 0$ to ∞. This can be used to replace the somewhat crude methods used to interpolate in Σ_0 in tables of Bondarenko self-shielded cross sections. Here you will find that you need fewer values of Σ_0 to tabulate data, and results will be smooth and continuous.

$$<\Sigma_R(\Sigma_0)> = \frac{\sum_B \Sigma_{RB} P_B /[\Sigma_t + \Sigma_0]}{\sum_B P_B /[\Sigma_t + \Sigma_0]}$$

The Intermediate Resonance (IR) Approximation

The **Probability Table Method** (PTM) uses the **Narrow Resonance** (NR) Approximation to sample from the entire distribution of cross sections after each scatter, so it is important for us to understand what this means and how it affects results. Here I will briefly describe the various resonance models, including Narrow (NR), Wide (WR), and Intermediate (IR), and investigate what effect these models have on our calculated results, and more importantly I will try to explain why. Returning to the 1-D Boltzmann equation,

$\mu\ \partial\Phi(E,z,\mu)/\partial z + \Sigma t(E,z)*\Phi(E,z,\mu) = R(E,z,\mu)$; here $R(E,z,\mu)$ is the slowing down and sources.

In an infinite, homogeneous medium this becomes,

$\Sigma t(E)*\Phi(E) = R(E)$
Total Reactions = Slowing Down Spectra

In the **Narrow Resonance** (NR) Approximation we assume that R(E) is smoothly varying with energy, e.g., at successfully higher energies R(E) is: Maxwellian, 1/E, fission, and fusion spectra. Obviously, since we assume R(E) is smoothly varying with energy, this equation says that the **Total Reaction Rate is smoothly varying**, and that the Flux ~ $1/\Sigma t(E)$, the classic self-shielding I have been discussing throughout this paper.

In the other extreme the **Wide Resonance** (WR) Approximation we assume that the slowing down varies following the cross section,

$\Sigma t(E)*\Phi(E) = \Sigma t(E)*R'(E)$
Total Reactions = Slowing Down Spectra

This equation says that the **Flux is smoothly varying**, and that the Flux is not self-shielded.

Briefly, the **Narrow Resonance** (NR) model assumes that the widths and spacings of the resonances in the medium are narrow compared to the range of secondary scattered energies, so there is a probability that any scattered neutron can "see" the entire range of cross sections. In the other extreme of **Wide Resonance** (WR) model assumes that the resonance, or energy dependence of the cross section is so wide compared to the range of scattered energies that after a collision the scattered neutron "sees" only the same cross section it saw before the collision.

In nature, when we examine the entire periodic table, we find almost a continuum of isotopes with various atomic weights, and resonance spacings and widths, that neither the narrow nor wide model is accurate in all cases; hence the need for the **Intermediate Resonance** (IR) model. A detailed description of the IR is beyond the scope of this paper; see the papers by Rubin Goldstein [27, 28, 29]. Soon after developing the Multi-Band model [10,11, 12], I realized that based on the many results we were calculating, the NR is not always accurate enough, so I extended the multi-band method by adding the IR Approximation to TART [13]. Here I will merely present a few example results based on the six cross section models used above and adding IR results (identified as Multi-Band NR and IR) in the results.

Note that when using **Continuous** energy cross sections in Monte Carlo none of these resonance width models/approximations are used, so we can use continuous energy results as a standard to determine which of these models are accurate – or inaccurate.

Infinite, Homogeneous Model: The first example should be the simplest possible, corresponding to the above equation for an infinite, homogeneous medium. I homogenized the Water/U system discussed above, for a range of ratios of H_2O **molecules** to U **atoms**, including five different ratios: 1:100, 10:100, 100:100, 1000:100, 10000:100, i.e. from predominately U (100 times more), to predominately H_2O (100 times more). In each case I first used continuous energy cross sections and adjusted the ^{235}U enrichment to make the system approximately critical. I then ran TART using each of the six cross section models discussed above, plus a seventh model to provide multi-band results using either narrow (NR) or intermediate (IR) resonance treatments. Each TART run used 10^{+8} neutron samples, to achieve converged results to within about 0.1% (3-digit convergence).

Infinite, Homogeneous: H_2O Molecules Atoms Ratio

Model	1:100	10:100	100:100	1000:100	10000:100
Continuous	0.999816	1.000080	1.000810	0.999657	1.000290
Multi-Group	0.966235	0.828187	0.794985	0.903417	0.987059
Multi-Band NR	1.000680	1.010940	1.023410	1.007310	0.999690
Multi-Band IR	1.000950	1.002020	1.000550	0.997719	0.998776
Unshielded	0.966169	0.828150	0.795056	0.903405	0.987063
Totally	0.999059	1.006050	1.090950	1.067940	1.027070
Partial	0.986059	0.935382	0.956772	0.997413	1.012270

Frankly I was shocked by the results; here is a summary of what I see from the above table,

1) The effects of the difference in self-shielding models are **most extreme near the middle of the table (100:100 ratio)**. For a much lower ratios the system becomes so heavily absorbing it is hard to see the effect of elastic scatter in the resonance range, and at much higher ratios the scatter is predominately from the water, particularly H, which scatters over such a large secondary energy range that it satisfies the narrow resonance (NR) model.
2) **Multi-group** and **Unshielded** results show incredible (at least to me), poor results; in the worst case predicting $K_{eff} \sim 0.795$, which is dangerously low if you are trying to predict the safety of a homogeneous mixture of materials; this result I found particularly surprising and SCARY!!!! Statistically these two models should – and do – produce very similar results; these results were so shocking I would not have believed them without this independent agreement.
3) **Totally** and **Partially** Shielded, respectively over (Totally ~ 1.091) and under (Partially ~ 0.956) predict Keff results.
4) In this case the **Multi-Band Narrow Resonance** (NR) results are even worse than the Totally or Partially shielded results (NR ~ 1.023); not surprising, since U is does not satisfy the Narrow Resonance model.
5) Only the **Multi-Band Intermediate Resonance** (IR) results produce close to acceptable results across all five H_2O to U ratios (at 100:100 ~ 1.0005).

Simple 1-D Planar Infinite Model: The below table is identical to Table 1 above, under a Simple 1-D Planar model, except that I have added Intermediate Resonance (IR) approximation models. In this case the difference between narrow resonance (NR) and intermediate resonance is only 0.000320 (~ 0.03 %), which is insignificant to the statistical accuracy of the results. **The bottom line is that for this simple 1-D model NR versus IR plays no significant role.**

U/Water Criticality Including Narrow (NR) and Intermediate (IR) Results

Cross Section Representation		Expected K-eff	Difference in K-eff	Removal Lifetime (Microsec.)	Median Energy (eV)	Seconds
Continuous		0.999924	--------	7.89162D+01	5.00948D-02	5066.660
Multi-Group		0.974683	-0.025241	7.70376D+01	5.01225D-02	3837.700
Multi-Band	NR	1.000980	0.001056	7.90684D+01	5.01097D-02	4404.120
Multi-Band	IR	1.001300	0.001376	7.90471D+01	5.00872D-08	4208.120
Unshielded		0.974645	-0.025279	7.70372D+01	5.01247D-02	4442.640
Totally Shielded		1.001750	0.001826	7.97356D+01	4.95769D-02	4581.800
Partial Shielded		0.991570	-0.008354	7.86170D+01	4.98773D-02	4512.280

Homogeneous versus Heterogeneous: Why is there such a significant difference between the preceding H_2O/U infinite, **homogeneous** system, and this H_2O/U finite, **heterogeneous** system? Because in the **homogenous** case the scatter was occurring in the entire uniform mix of materials, so that for some H_2O/U ratios the scatter from the U was important but did not satisfying the narrow resonance (NR) model. In the **heterogeneous** case the scatter and slowing down was primarily in the H_2O, which does satisfy the NR model. In the heterogeneous case what is important is not the scatter within the U, but rather the all-important boundary conditions at the H_2O to U interface; here the spectrum of neutrons incident from the H_2O into the U is smooth from scatter in H_2O and satisfies the narrow resonance model (NR).

The **Probability Table Method** (PTM) [24, 25], using the narrow resonance (NR) model in the unresolved resonance region has been more successful than you might think, even though most heavy even-odd isotopes (fuels), themselves do not narrow resonance (NR) scatter. As long as it is dealing with **heterogeneous** media where the slowing down is primarily outside of the fuel what is most important is not the scatter inside the fuel, but rather the boundary conditions to introduce neutrons into the fuel with the "correct" distribution of cross sections; hopefully this is illustrated by the above figures showing the energy and spatial dependence of the uncollided flux into the U from the H_2O.

The above two examples are for infinite homogeneous and heterogenous media, which being infinite are of course completely theoretical. To illustrate the differences between Narrow and Intermediate Resonance Models for real systems, below I present results for the Uranium Slow Critical Assemblies where using the Narrow Resonance Model we found small, but significant, differences for assemblies 207 through 231.

Uranium Slow Critical Assemblies: Below is a comparison for the Uranium Slow Critical Assemblies 207 through 231. These are the assemblies where we found significant differences using the Narrow Resonance (NR) Model; below the Narrow Resonance (NR) results are compared to Intermediate Resonance (IR) Model results. The results show that for these assemblies using the Intermediate Resonance (IR) reduces the difference to within 0.1%, except for one case (225) where it is 0.11% (statistically the same as 0.1%).

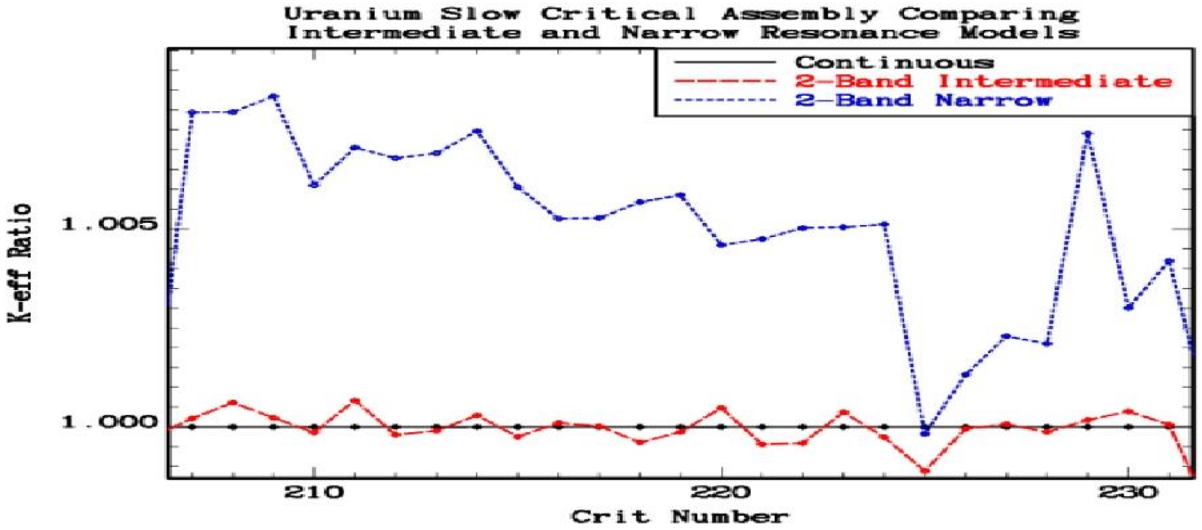

Critical Assembly			Intermediate Resonance		Narrow Resonance	
207	LCT006-1 U235	Water	207	1.0002102	207	1.0079426
208	LCT006-2 U235	Water	208	1.0006123	208	1.0079456
209	LCT006-3 U235	Water	209	1.0002300	209	1.0083485
210	LCT006-4 U235	Water	210	0.9998600	210	1.0060991
211	LCT006-5 U235	Water	211	1.0006700	211	1.0070495
212	LCT006-6 U235	Water	212	0.9998001	212	1.0067855
213	LCT006-7 U235	Water	213	0.9999000	213	1.0069066
214	LCT006-8 U235	Water	214	1.0002898	214	1.0074652
215	LCT006-9 U235	Water	215	0.9997503	215	1.0060522
216	LCT006-10 U235	Water	216	1.0000999	216	1.0052534
217	LCT006-11 U235	Water	217	1.0000200	217	1.0052721
218	LCT006-12 U235	Water	218	0.9996105	218	1.0056730
219	LCT006-13 U235	Water	219	0.9998701	219	1.0058548
220	LCT006-14 U235	Water	220	1.0004792	220	1.0045922
221	LCT006-15 U235	Water	221	0.9995608	221	1.0047417
222	LCT006-16 U235	Water	222	0.9995907	222	1.0050217
223	LCT006-17 U235	Water	223	1.0003694	223	1.0050425
224	LCT006-18 U235	Water	224	0.9997404	224	1.0051126
225	LMT001 U-nat	D2O	225	0.9988893	225	0.9998243
226	LMT002-1 U235	D2O	226	0.9999504	226	1.0013182
227	LMT002-2 U235	D2O	227	1.0000700	227	1.0022889
228	LMT002-3 U235	D2O	228	0.9998713	228	1.0020988
229	LMT002-6 U235	D2O	229	1.0001731	229	1.0074080
230	LMT002-10 U235	D2O	230	1.0003893	230	1.0030043
231	LMT002-11 U235	D2O	231	1.0000580	231	1.0041909

Lawrence Livermore National Laboratory
Technical Information Department
Livermore, CA 94551